JOURNAL OF GEOPHYSICAL RESEARCH, VOL. 95, NO. B10, PAGES 15,893–15,910, SEPTEMBER 10, 1990

Basaltic Melt Evolution of the Hengill Volcanic System, SW Iceland, and Evidence for Clinopyroxene Assimilation in Primitive Tholeiitic Magmas

REIDAR G. TRØNNES[1]

Nordic Volcanological Institute, University of Iceland, Reykjavík

The thick oceanic crust of Iceland is formed by tholeiitic central volcanoes arranged in en echelon patterns along the 40–50 km wide rift zones. The Hengill central volcano in the southwestern rift zone has produced 25–30 km^3 of hyaloclastites and lava during the last 0.11 m.y., with maximum productivity during the isostatic rebound following the degalciations 0.13 and 0.01 m.y. ago. The eruption units cover a compositional spectrum from picrite to rhyolite, but the volume of andesite, dacite, and rhyolite is small. The petrographic relations of pillow rim and hyaloclastite glass indicate that the basaltic melts were saturated with olivine and plagioclase, except for the most primitive ones that were undersaturated with plagioclase. Saturation with clinopyroxene was reached in some of the intermediate and evolved basaltic melts. Corroded and partly resorbed crystals of clinopyroxene and partly disintegrated gabbro nodules with resorbed clinopyroxene indicate that selective assimilation contributed to the evolution of the most primitive melts. The intermediate and evolved basaltic glass compositions fall along the low-pressure cotectic for mid-ocean ridge basalt (MORB) compositions saturated with olivine, plagioclase, and clinopyroxene, but the primitive glasses (9–9.7 wt % MgO) fall well inside the low-pressure olivine + plagioclase primary phase volume. The primitive Hengill glasses have significantly higher CaO and lower Al_2O_3 than primitive glasses from oceanic spreading centers. Their low pressure undersaturation with respect to clinopyroxene and the absence of clinopyroxene phenocrysts indicate that they are not parental to the intermediate Hengill basalts, since fractionation modelling requires a large proportion of clinopyroxene in the fractionating assemblage. The most primitive melts could be produced by fractionation of olivine and plagioclase combined with 5–30 % assimilation of clinopyroxene, and the intermediate melts could be derived by mainly olivine and plagioclase fractionation, from melts equilibrated with peridotitic residues at pressures of 1–2 GPa. The further evolution of the basaltic spectrum can be explained by fractionation of olivine, plagioclase, and clinopyroxene combined with minor contamination by anatectic crustal melts. The rate of magma supply from the mantle to the crust is controlled by the isostatic conditions and is very low in periods of glacial loading of the crust. This leads to infrequent and small eruptions of dominantly evolved magmas. The dense picritic magmas (9–9.7 wt % MgO in the glass phase) were driven to the surface by magmatic overpressure in the mantle at an early deglaciation stage characterized by the absence of large, trapping magma chambers in the lower crust. The assimilation of clinopyroxene in these melts could proceed by direct contact with the solidified cumulate sequences and gabbro intrusions. Clinopyroxene assimilation in combination with olivine fractionation may also contribute to the chemical evolution of some of the most primitive MORB magmas.

INTRODUCTION

The crustal formation along the Icelandic rift zones is characterized by higher volcanic productivity than along other segments of the Mid-Atlantic ridge [*Imsland*, 1983; *Vink*, 1984; *Oskarsson et al.*, 1985]. The high magma production is caused by an anomalously hot mantle beneath Iceland, and an "Icelandic mantle plume" has been defined on the basis of basalt geochemistry [*Schilling*, 1973] and seismic structure of the mantle [*Tryggvason et al.*, 1983]. The resulting crust along the track of the mantle plume (the Greenland-Iceland-Faerö transverse ridge) is much thicker than normal oceanic crust [*Bott and Gunnarsson*; 1980; *Björnsson*, 1984].

Pálmason [1973, 1986] and *Oskarsson et al.* [1982, 1985] proposed simplified dynamic and petrogenetic models for the crustal accretion in Iceland. The loading of volcanic products onto the rift zone crust is accompanied by isostatic subsidence, and progressive dehydration and partial melting may occur in the downgoing lava pile at depths of 3-6 km. Below 5-6 km depth the crust is most likely dominated by the magmatic infrastructure resulting from melt injections from the mantle and may be similar to the cumulate sequences of ophiolites.

Tholeiitic volcanic systems of the active rift zones are the main processing units of the crustal accretion in Iceland. These systems evolve over time from incipient fissure swarms to central volcanoes characterized by the presence of shallow intrusive bodies, rhyolites, and high-temperature geothermal fields. Information about the nature and dynamics of magma injections from the mantle, crustal magma differentiation, and eruptions at the surface is fundamental to an understanding of the accretion processes of the volcanic systems.

The Hengill volcanic system in southwestern Iceland offers such insight and was chosen for a systematic study of the variation in melt composition between and within the various eruptive units produced during the last 0.1 m.y. Located near the intersection of three volcanic and tectonic zones (Figure 1) the system has reached an intermediate stage of the evolution toward a mature central volcano. Whereas some of the central volcanoes have developed calderas and associated silicic pyroclastic deposits, the Hengill system lacks these features, but contains minor volumes of rhyolites.

[1]Now at C.M. Scarfe Laboratory of Experimental Petrology, Department of Geology and Institute of Earth and Planetary Physics, University of Alberta, Edmonton, Canada.

Paper number 90JB00312.
0148-0227/90/90JB-00312$05.00

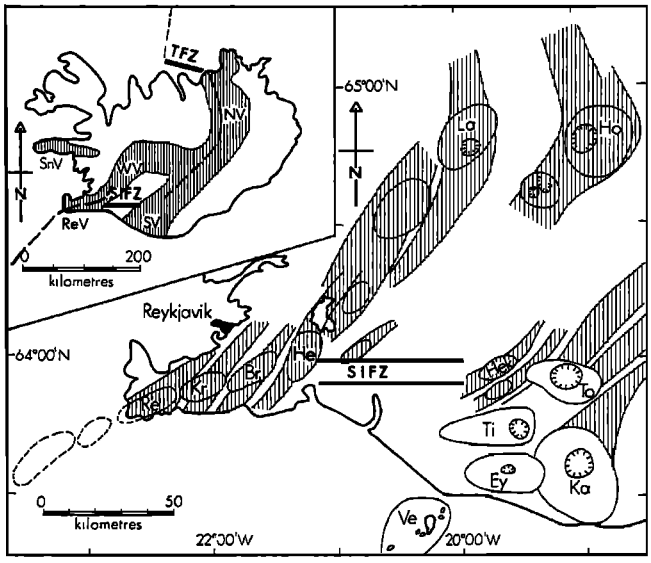

Fig. 1. Inset map: The volcanic zones in Iceland are shaded. Active rift zones with tholeiitic volcanism: Reykjanes Volcanic Zone (ReV), Western VZ (WV), and Northern VZ (NV). Non-rifting zones with transitional to alkaline volcanism: Southern VZ (SV) and Snæfellsnes VZ (SnV). The Tjörnes Fracture Zone (TFZ) offsets the oceanic spreading center north of Iceland from the Northern Volcanic Zone. The South Iceland Fracture Zone (SIFZ) connects the southern tip of the active rift zone in eastern central Iceland with the rift zone on the Reykjanes peninsula (ReV). Main map: The rifting volcanic systems (central volcanoes, some of them with calderas, and associated southwest-northeast trending dike and fissure swarms) are shaded: Re, Reykjanes; Kr, Krísuvík; Br, Brennisteinsfjöll; He, Hengill; La, Langjökull; Ho, Hofsjökull; and Hek, Hekla. Nonrifting central volcanoes: To, Torfajökull; Ti, Tindafjallajökull; Ey, Eyafjallajökull; Ka, Katla; and Ve, Vestmannaeyjar. The hatched circles within volcanic centres are calderas. Based on work by *Sæmundsson* [1979].

The immature volcanic systems farther west along the Reykjanes peninsula represent a transition to the thinner oceanic crust along the submarine Reykjanes Ridge. In spite of the thicker crust beneath Hengill and the lack of rhyolites in the western Reykjanes fissure swarms, the relationships between melt evolution, volcanic productivity, and timing of the upper Pleistocene eruption events are comparable in the two areas [*Jakobsson et al.*, 1978; *Gudmundsson*, 1986] A petrogenetic model of magma fractionating and interacting with the crust at different levels is proposed to explain the melt evolution of the Hengill system. The process of resorption of clinopyroxene, observed both texturally and chemically in the most primitive glasses, may also have important implications for the early melt evolution at submarine oceanic spreading centers.

GEOLOGY

The Postglacial activity of the volcanic systems of the Reykjanes peninsula (Figure 1) falls into three stages [*Jakobsson et al.*, 1978]: (1) small picritic lava shields (2) larger (up to 7 km^3) olivine tholeiitic shields and (3) lava flows erupted from fissure swarms.

The eruption rate was high in a short period just after the deglaciation and then declined. In each volcanic system the lava shields are located on the margins of the central fissure swarm. Broadly similar field relations are observed in the Hengill system where the main central volcanic complex is surrounded by interglacial and early postglacial lava shields, as well as picritic and primitive olivine tholeiitic eruption units (Figure 2).

Sæmundsson [1967] provided a detailed account of the geology of the Hengill central volcano, and recent work associated with geothermal exploration is summarized by *Arnason et al.* [1986] and *Fougler* (1988a,b]. The Hengill area has hosted a central volcano since the early Matuyama geomagnetic epoch [2.5-0.7 Ma). In early Brunhes the volcanic center shifted 5-10 km toward northwest from an original position at Grændalur to the present location [*Björnsson et al.*, 1974]. According to *Arnason et al.* [1986] the upper Pleistocene and Postglacial (0.7 Ma to present) activity has been confined to two parallel volcanic systems with centers in the Hengill massif and a mountain massif 5 km farther east. Although both subsystems have been active throughout the last glacial period (Weichsel, 0.11-0.01 Ma), it seems that the eastern subsystem developed earlier than the western subsystem [*Arnason et al.*, 1986].

The upper Pleistocene eruptive products comprise mainly subaquatic (and subglacial) hyaloclastites in the form of pillow lavas, pillow breccias, and tuffs. These deposits are mostly confined to ridges and elongated bodies parallel to the NE trending fault and fissure system. Some are capped with plateaus of subaerial lava flows, e.g., the Hengill table

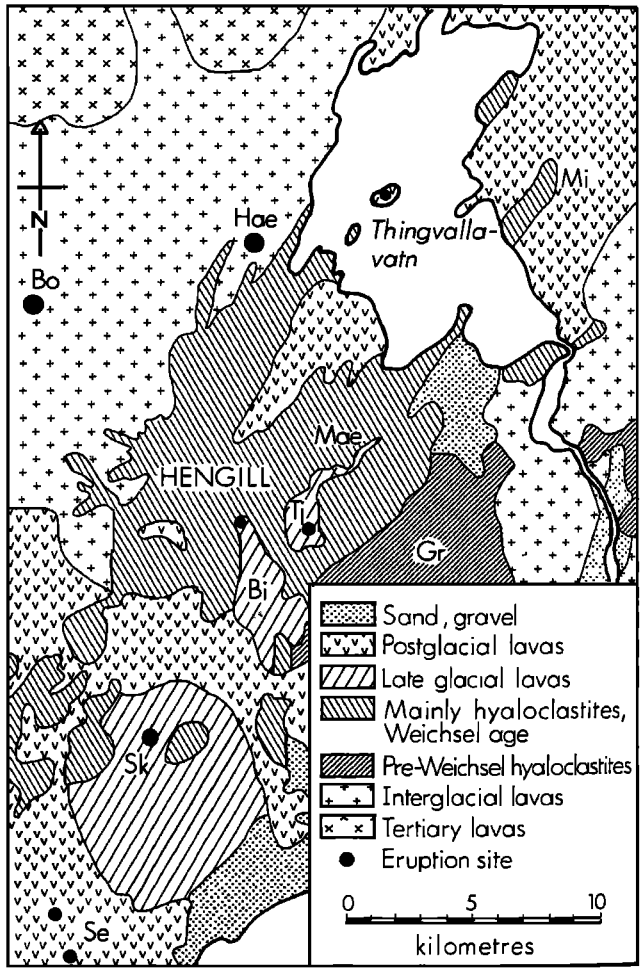

Fig. 2. Simplified geological map of the central portions of the Hengill volcanic system. Older volcanic centre at Grændalur (Gr); interglacial shield volcanoes: Borgarhólar (Bo) and Hædir (Hae); late glacial picritic eruption units: Midfell (Mi) and Mælifell (Mae); late glacial lava flows and lava shields: Tjarnarhnúkur (Tj), Bitra (Bi) and Skálafellsdyngja (Sk); Postglacial lava shields: Selvogsheidi (Se). Based on work by *Sæmundsson and Einarsson* [1980].

mountain. *Arnason et al.* [1986] ascribe the Hædir and Borgarhólar lava shields west of Hengill to the last interglacial period. The presently exposed hyaloclastites of the western subsystem stratigraphically overlie the shield lavas and were therefore formed during Weichsel. The estimated total volume of these hyaloclastites is 14-18 km³ [*Arnason et al.*, 1986]. The corresponding eruptive units in the eastern subsystem are of considerably smaller volume, probably less than 10 km³. Late glacial and Postglacial lava shields (Bitra, Skálafellsdyngja, and Selvogsheidi) contribute an additional 5-10 km³ in the southern parts of the Hengill volcanic system. Five or six Postglacial eruptions from the fissure swarm associated with the western subsystem have produced about 0.5 km³ of lava.

PETROGRAPHY

This study concerns the exposed eruption units of Weichsel and Holocene age. All of the major units within both of the subsystems were sampled. In order to study the compositional variation within the eruptive units, most of the units were also sampled at several locations. Special care was taken to obtain fresh volcanic glass in the form of pillow rims, sideromelane fragments in tuffs, and scoria from the Postglacial lava flows.

The types and morphologies of the phenocrysts correspond largely to those in other basaltic glasses from Iceland [*Makipaa*, 1978] and from the FAMOUS area of the Mid-Atlantic Ridge [*Bryan*, 1979, 1983]. Plagioclase and olivine dominate the phenocryst assemblage. Clinopyroxene is present in small amounts as Al- and Cr-rich endiopside [*Hardardóttir*, 1983, 1986; *Risku-Norja*, 1985] in the most magnesian glasses (MgO > 8.9 wt %) and as augite in a few of the more differentiated samples (MgO < 6.0 wt %). The Al-Cr-endiopside occurs in gabbro nodules and as large and partly resorbed phenocrysts (Figure 3), whereas augite mostly occurs as microphenogrysts and often in glomerophyric bow-tie intergrowths with plagioclase. *Bryan* [1979] interpreted the latter texture as an indication of cotectic crystallization of plagioclase and clinopyroxene. Spinel occurs only in the most MgO-rich samples as inclusions (often euhedral) in olivine and Cr-diopside and as separate small euhedral-subhedral crystals in the glass.

As discussed by *Bryan* [1979] and recently documented by *Lipman et al.* [1985] microphenocrysts may be a result of syneruptive crystallization due to for instance a sudden loss of volatiles from the magma. The glass composition of samples with a significant amount of microphenocrysts may therefore not represent fully the melt composition prior to the eruption process. During the study of the glass compositions, altered glass and glass containing more than about 5 vol % microphenocrysts were avoided.

Table 1 gives the average phenocryst content within four compositional groups of basaltic glasses. The table shows that the total phenocrysts content decreases with increasing melt differentation (decreasing MgO content). Large amounts of olivine phenocrysts, accompanied by spinel and corroded Al-Cr-endiopside xenocrysts, are found only in picritic samples with more than 8.9 wt % MgO in the glass phase, whereas the most differentiated samples with less than 4.0 wt % MgO are aphyric.

TABLE 1. Average Phenocryst Content in Four Compositional Groups of Basaltic Glasses

MgO			Olivine		Plagioclase	
Range, wt %	N	X_{MgO}	Ph	Mi	Ph	Mi
>8	10	8.9	11.9	*	2.9	*
8 - 7	37	7.5	1.1	*	9.0	1.0
7 - 6	34	6.5	1.5	*	6.5	1.5
<6	22	5.2	*	*	2.6	1.0

N, number of samples within the groups; X_{MgO}, average MgO content (wt %) within the groups; Ph, phenocryst; Mi, microphenocryst. The four most MgO-rich samples contain small amounts of corroded Cr-diopside xenocrysts and spinel, and some of the more differentiated samples contain small amounts of augite.

*Less than 1.0 vol%.

Some of the eruptive units in the eastern subsystem have large amounts (20-30%) of plagioclase phenocrysts. This applies in particular to a NNE trending zone including the youngest hyaloclastite ridges in the area, as well as a late glacial lava flow from Tjarnarhnúkur (Figure 2) which also contains large amounts of partly disintegrated gabbro nodules with cumulus plagioclase and intercumulus clinopyroxene (Figure 4). In spite of the disintegration of the gabbro nodules, the Tjarnarhnúkur lava is devoid of clinopyroxene phenocrysts. The two most magnesian eruption units, Mælifell and Midfell, are also confined to the eastern subsystem (Figure 2). In addition to the abundant olivine

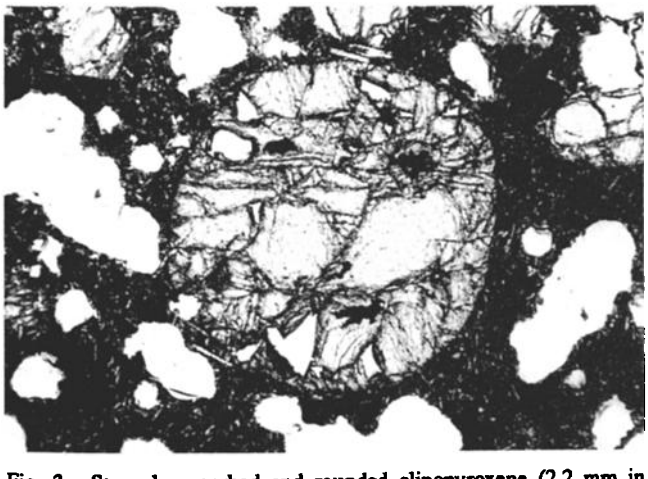

Fig. 3. Strongly resorbed and rounded clinopyroxene (2.2 mm in diameter) in sample 71 (see Table 2) from the late glacial Mælifell eruption unit.

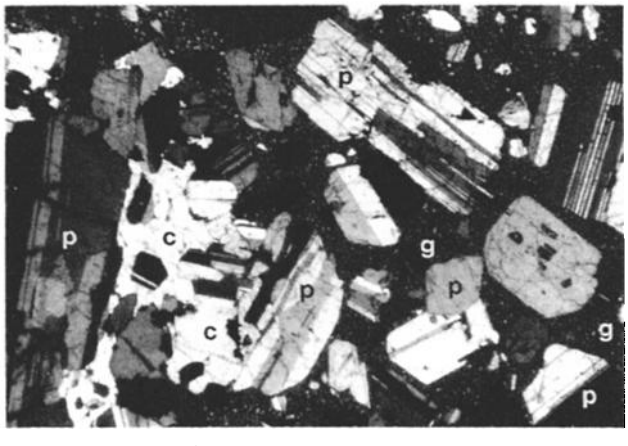

Fig. 4. Partly disintegrated gabbro nodule in a strongly plagioclasephyric lava from the late glacial Tjarnarhnúkur eruption unit (field of view 6 x 10 mm). Note the presence of large clinopyroxenes in the nodule (left) but no clinopyroxene phenocrysts in the lava (right). c, clinopyroxene; p, plagioclase; g, groundmass.

phenocrysts in these picritic units, the Midfell unit also contains gabbroic cumulate nodules with plagioclase, Al-Cr-endiopside, and olivine [*Risku-Norja*, 1985].

PHENOCRYST COMPOSITION

Hardardóttir [1983, 1986] report mineral composition of phenocrysts in a series of rock types of the Hengill volcanic system. Additional analyses of gabbro nodule minerals and phenocrysts from the Midfell eruption unit are given by *Risku-Norja* [1985]. Some additional analyses, especially of the gabbroic cumulate nodules in the Tjarnarhnúkur lava flow, were collected as part of this study. Representative phenocryst compositions used in least squares mass balance calculations of fractionation and assimilation are listed in Table 2.

Although minor intrasample variation in phenocryst composition occurs, most of the basaltic eruption units have remarkably homogeneous phenocrysts populations. Even plagioclase, which has very low chemical diffusivity [*Morse*, 1982], lacks pronounced zoning in most of the eruption units. The lack of major chemical zoning indicates that the phenocrysts in each of the eruption units have grown during periods when the melt compositions were kept nearly constant.

Most of the plagioclase phenocrysts of the eruption units in the eastern part of the Hengill system have similar compositions to the plagioclase crystals in the gabbroic cumulate nodules of the Midfell and Tjarnarhnúkur units. The partly resorbed Al-Cr-endiopside megacrysts (Figure 3) in the Mælifell and Midfell picrites corresponds completely to the clinopyroxene in the Midfell nodules, whereas the endiopside

TABLE 2. Phenocryst Compositions Used in Least Squares Mixing Calculations

Plagioclase	SiO_2	Al_2O_3	Fe_2O_3	CaO	Na_2O	K_2O	An%
104	47.5	33.5	0.68	16.5	2.01	0.03	82.2
Tj	47.6	33.2	0.64	16.5	1.74	0.03	84.3
Tj	46.8	33.6	0.62	17.1	1.61	0.04	85.5
H2	47.6	32.2	0.58	17.2	1.59	0.03	85.1
H6a	47.5	32.3	0.68	17.0	1.69	0.03	84.3
H6b	48.4	32.3	0.65	16.8	1.75	0.02	83.8
H6c	51.9	29.5	0.98	13.9	3.34	0.05	69.1
H7	48.5	32.3	0.59	16.8	1.67	0.02	84.5
H8a	47.2	32.6	0.68	17.7	1.38	0.02	84.1
H8b	47.5	32.5	0.62	16.7	2.23	0.03	79.9
H11	47.5	32.7	0.58	17.2	1.50	0.01	86.1
H12	47.3	33.3	0.71	16.9	1.78	0.04	84.0
H15a	47.6	32.9	0.68	16.8	1.79	0.03	83.8
H15b	50.4	30.9	0.77	14.6	2.94	0.07	73.3

Olivine	SiO_2	FeO	MnO	MgO	CaO	NiO	Fo%
73	40.9	10.1	0.14	48.4	0.24	0.26	89.5
74	38.8	20.0	0.29	40.8	0.09	0.11	78.4
105	39.2	17.0	0.27	43.1	0.12	0.20	81.9
106	40.6	10.8	0.16	48.2	0.26	0.26	88.8
118	39.6	15.4	0.24	43.7	0.13	0.26	83.5
119	39.2	16.1	0.22	43.6	0.14	0.24	82.9
H2	38.4	20.4	0.32	40.8	0.30	0.17	78.2
H6	38.5	18.4	0.29	41.7	0.27	0.12	80.2
H7	38.2	21.2	0.31	40.1	0.27	0.12	77.2
H8	39.0	15.3	0.25	44.3	0.34	0.18	83.8
H11b	39.9	10.6	0.14	48.8	0.36	0.21	89.1
H11c	39.5	13.0	0.18	46.3	0.29	0.18	86.4
H12	38.7	19.9	0.30	41.9	0.32	0.18	79.0
H15a	38.5	19.2	0.34	42.1	0.30	0.10	79.6
H15b	37.2	26.8	0.38	35.4	0.32	0.13	70.2

Clinpyroxene	SiO_2	TiO_2	Al_2O_3	FeO	MnO	MgO	CaO	Na_2O
Tj	52.8	0.37	2.68	5.71	0.15	16.4	21.2	0.21
H2	51.9	0.80	2.80	7.80	0.18	16.0	19.8	0.30
H6	50.8	0.78	3.31	7.57	0.20	16.2	19.3	0.23
H11*	50.9	0.26	4.54	4.31	0.09	16.8	21.0	0.20
H15	51.2	0.83	3.42	7.44	0.16	16.3	19.4	0.28

Sample numbers beginning with H are averages of representative phenocryst analyses of samples H2, H6, H7, H8, H11 and H15 by *Hardardóttir* [1983]. Different compositional populations are marked as a, b, and c. Minerals in the gabbro nodules of the Tjarnarhnúkur lava flow (Tj) and numbers without letters are analyses from the present study.

*Contains 1.13 wt % Cr_2O_3.

in the nodules of the Tjarnarhnúkur lava is higher in Si and Fe and lower in Al and probably Cr.

GLASS COMPOSITION

Major Elements

The composition of the glass phase of the main picritic and basaltic eruption units of the Hengill system is given in Table 3, and the analytical procedures are outlined in the Appendix. Although the upper Pleistocene hyaloclastites includes minor amounts of tholeiitic andesite (icelandite), dacite, and rhyolite, the major element compositions of only the basaltic glasses are treated in this paper. Even the most evolved sample reported in Table 3 (sample 46: 53.4 wt % SiO_2, 3.35 wt % MgO) falls within the basaltic range based on the classification of *Irvine and Barager* [1971]. However, according to the classifications of *Carmichael et al.* [1974] and *Basaltic Volcanism Study Project* [1981] based on SiO_2 content this evolved sample falls within the basaltic andesite range.

The MgO content is generally the most sensitive indicator of chemical variation in basaltic suites, and was chosen as the abscissa of the variation diagrams in Figure 5. The following covariations can be observed:

CaO is strongly, and Al_2O_3 is less markedly, positively correlated with MgO, possibly indicating a combined olivine, plagioclase and clinopyroxene fractionation.

K_2O, Na_2O, P_2O_5, FeO (total Fe) and TiO_2 all increase with increasing degree of evolution (decreasing MgO).

TABLE 3. Major Element Composition of Basaltic Glasses.

No.	Coordinates* UTM 27	SiO_2	TiO_2	Al_2O_3	FeO^+	MnO	MgO	CaO	Na_2O	K_2O	P_2O_5
1	831057	48.1	2.24	13.9	12.4	0.24	6.58	12.0	2.52	0.29	0.26
2	846066	47.4	2.01	15.2	11.6	0.19	7.55	12.7	2.51	0.31	0.25
3	844065	47.1	2.49	13.7	12.7	0.22	6.79	12.2	2.43	0.30	0.28
4	839052	47.4	2.45	13.7	12.8	0.23	6.92	12.3	2.44	0.26	0.28
5	819113	49.1	1.69	14.1	12.1	0.21	7.29	12.7	2.56	0.18	0.18
7	825045	48.7	2.60	13.9	12.4	0.23	6.12	11.3	2.84	0.45	0.32
8	820043	48.5	2.36	13.8	12.7	0.19	6.60	12.3	2.66	0.32	0.29
12	866143	48.4	2.31	13.5	12.5	0.23	6.30	11.8	2.63	0.44	0.32
14	850133	48.0	2.52	13.6	12.4	0.23	6.27	12.1	2.80	0.39	0.27
15	858130	49.5	2.18	13.9	12.1	0.23	6.30	11.3	2.73	0.42	0.43
16	864132	48.9	2.31	13.8	12.2	0.19	6.29	11.8	2.78	0.36	0.29
18	865135	48.5	2.30	13.7	12.4	0.18	6.33	12.0	2.73	0.38	0.34
19	872142	48.5	2.22	13.6	12.6	0.25	6.25	11.4	2.78	0.34	0.33
20	871121	48.4	2.57	13.6	12.9	0.21	6.02	11.7	2.77	0.43	0.33
22	891105	48.9	1.38	14.2	11.2	0.20	7.70	13.3	2.26	0.12	0.12
23	879147	48.1	2.46	13.3	14.2	0.18	5.91	11.3	2.72	0.41	0.30
26	885120	48.5	1.60	13.8	12.3	0.21	7.02	12.4	2.07	0.21	0.23
29	905110	48.5	2.11	13.8	13.2	0.17	6.24	11.3	2.52	0.29	0.21
30	856086	50.1	2.24	13.9	13.6	0.14	5.86	11.3	2.72	0.43	0.32
31	854099	48.0	2.81	13.4	13.8	0.16	5.81	11.4	2.64	0.40	0.36
32	849105	48.7	2.18	13.5	12.6	0.15	6.42	12.2	2.50	0.31	0.32
33	847105	47.7	2.16	14.0	12.3	0.18	6.28	11.9	2.49	0.42	0.24
34	847099	48.6	2.22	13.9	12.5	0.15	6.40	12.2	2.55	0.32	0.22
35	848092	47.9	2.57	13.8	13.1	0.17	6.13	12.1	2.58	0.42	0.23
36	852088	48.8	2.65	13.4	13.8	0.15	5.92	11.3	2.57	0.38	0.28
38	899047	48.1	2.68	14.9	13.0	0.16	6.10	10.8	2.83	0.46	0.28
41	900053	47.4	2.60	14.2	12.5	0.18	6.46	11.2	2.58	0.41	0.28
42	910046	48.8	2.17	14.3	11.2	0.17	6.68	11.7	2.48	0.49	0.28
44	915052	48.9	1.69	14.8	10.5	0.14	7.25	12.8	2.24	0.40	0.25
46	916074	53.4	2.81	13.0	14.2	0.20	3.35	7.83	2.89	0.87	1.03
45	917068	48.5	2.45	13.9	12.2	0.14	6.63	12.5	2.52	0.33	0.27
47	814025	47.7	1.81	14.8	11.1	0.18	7.91	12.8	2.15	0.23	0.19
49	818032	47.4	2.07	15.7	11.5	0.18	7.59	12.2	2.41	0.33	0.25
50	819019	48.3	2.44	14.2	12.5	0.22	6.50	11.6	2.63	0.44	0.28
51	817998	49.6	1.69	14.7	11.3	0.20	7.55	12.4	2.46	0.17	0.16
52	822021	48.0	1.55	15.1	10.8	0.20	8.15	12.7	2.21	0.19	0.20
53	836040	48.6	1.68	14.7	11.4	0.24	7.94	12.7	2.25	0.19	0.19
60	884081	48.4	2.45	13.8	12.7	0.23	6.46	12.7	2.75	0.42	0.35
61	888074	49.2	1.33	14.2	10.7	0.18	7.82	13.4	2.19	0.12	0.11
62	890072	48.6	1.32	14.3	10.8	0.22	7.77	13.2	2.26	0.12	0.15
63	891069	48.0	2.70	13.9	12.4	0.21	6.35	11.7	2.73	0.44	0.31
64	900071	48.4	1.56	14.4	10.9	0.19	7.64	13.2	2.36	0.16	0.15
65	900080	48.6	0.87	14.7	8.75	0.16	9.19	15.4	1.74	0.02	0.05
66	901084	48.1	0.82	14.9	8.89	0.16	9.34	15.1	1.77	0.02	0.06
67	900087	49.0	1.30	14.1	11.3	0.18	7.41	13.5	2.33	0.11	0.13
68	895087	47.5	2.08	13.8	12.7	0.19	6.54	11.8	2.75	0.27	0.23
69	880085	48.1	2.34	14.0	12.2	0.17	6.25	11.6	2.53	0.42	0.33

TABLE 3. (continued).

No.	Coordinates* UTM 27	SiO_2	TiO_2	Al_2O_3	FeO^+	MnO	MgO	CaO	Na_2O	K_2O	P_2O_5
70	879085	47.8	2.32	13.9	12.2	0.21	6.24	11.7	2.53	0.40	0.32
71	909091	48.5	0.97	14.8	9.19	0.20	8.88	15.3	1.84	0.01	0.08
72	909094	52.8	2.69	13.6	12.7	0.24	4.31	8.84	2.67	0.77	0.53
73	908095	48.0	0.98	14.9	9.52	0.19	8.98	15.4	1.82	0.01	0.06
74	911106	47.6	2.80	13.3	12.6	0.23	5.86	11.7	2.60	0.48	0.38
75	951134	48.8	1.33	13.5	11.4	0.19	7.28	13.5	2.30	0.10	0.13
76	938118	49.2	1.29	14.7	10.8	0.21	7.64	13.4	2.16	0.10	0.13
77	927091	49.5	1.33	14.1	11.3	0.21	7.40	13.4	2.24	0.13	0.14
78	843028	48.2	1.79	14.6	11.2	0.20	7.81	12.8	2.22	0.20	0.18
79	836065	48.8	2.43	13.5	12.8	0.23	6.71	12.2	2.54	0.27	0.28
80	828071	49.0	1.00	14.9	9.46	0.16	8.46	14.3	2.10	0.06	0.11
81	830070	48.8	1.02	14.7	9.41	0.19	8.45	14.4	2.09	0.06	0.10
82	832070	50.0	2.08	13.5	12.7	0.25	5.97	10.8	2.87	0.38	0.26
84	863045	49.4	1.55	14.0	11.6	0.22	7.29	12.7	2.47	0.13	0.11
86	862044	49.1	1.52	13.7	11.9	0.22	7.40	12.8	2.45	0.13	0.22
88	865124	50.7	2.57	13.3	13.9	0.29	4.55	9.21	2.70	0.75	0.81
89	870132	50.4	2.42	14.0	13.1	0.29	5.31	10.0	2.96	0.59	0.63
90	930087	51.9	3.18	13.0	14.3	0.29	3.67	8.11	3.29	0.78	0.79
91	929073	49.1	3.43	12.9	14.9	0.27	4.69	9.83	3.12	0.59	0.48
92	925064	48.6	3.25	13.2	13.9	0.26	5.23	10.6	3.01	0.61	0.46
93	932058	49.7	3.35	13.1	14.4	0.27	4.64	9.47	2.48	0.80	0.60
94	936065	49.4	1.02	14.4	9.80	0.17	8.52	14.6	2.03	0.02	0.09
96	934063	48.6	3.26	13.1	13.8	0.28	5.22	10.4	3.17	0.57	0.48
97	923062	48.7	3.07	13.1	14.0	0.23	5.18	10.7	2.80	0.62	0.42
98	757999	48.5	2.06	14.7	12.1	0.22	7.40	12.4	2.53	0.19	0.21
99	744984	48.8	1.90	14.0	12.0	0.20	7.42	12.5	2.34	0.15	0.20
100	794954	49.1	1.69	14.8	11.7	0.25	7.14	12.7	2.53	0.19	0.14
102	786942	48.3	2.18	15.0	11.5	0.20	7.19	12.0	2.52	0.35	0.36
103	781936	47.7	2.20	15.0	11.5	0.18	7.23	12.2	2.53	0.36	0.33
104	774928	49.7	1.89	14.1	12.4	0.22	6.84	12.4	2.47	0.24	0.26
105	755910	49.1	2.27	13.9	12.6	0.20	6.77	12.1	2.67	0.34	0.36
106	773974	49.5	1.55	13.8	10.9	0.14	7.45	13.9	2.18	0.15	0.15
107	777990	50.1	2.58	14.0	10.9	0.20	7.32	13.0	2.35	0.42	0.16
108	809992	49.4	1.61	14.0	11.9	0.24	7.39	12.8	2.32	0.10	0.19
109	883991	49.2	3.16	13.2	15.0	0.24	5.83	11.2	2.29	0.43	0.35
111	846962	49.3	1.70	14.6	11.2	0.16	7.47	12.3	2.48	0.24	0.19
113	808953	47.8	1.70	14.7	11.2	0.20	7.80	12.6	2.30	0.17	0.22
118	963211	48.7	2.07	14.7	11.0	0.21	7.28	12.6	2.34	0.21	0.25
119	967219	49.0	2.08	14.5	10.9	0.20	7.24	12.6	2.37	0.19	0.26
120	878132	48.8	2.78	13.4	13.5	0.20	5.87	11.1	2.76	0.40	0.31
121	880123	48.9	2.04	13.9	11.6	0.18	7.04	12.5	2.49	0.24	0.15
122	882118	50.6	3.01	13.5	13.3	0.24	4.95	9.59	2.79	0.68	0.54
123	899141	50.1	3.08	13.5	13.5	0.23	5.01	9.58	2.97	0.68	0.55
125	870090	48.2	3.40	12.9	15.3	0.24	4.85	10.4	2.87	0.50	0.37
126	873065	48.7	1.26	14.2	11.0	0.18	7.75	13.7	2.38	0.09	0.12
127	873063	49.3	1.28	14.4	10.8	0.18	7.66	13.4	2.32	0.08	0.13
130	898153	48.6	2.49	13.8	12.7	0.18	6.43	12.2	2.71	0.39	0.28
131	845072	48.0	2.51	13.8	13.1	0.20	7.07	12.4	2.49	0.27	0.27
132	848072	47.9	2.50	13.9	12.9	0.20	6.99	12.3	2.52	0.27	0.27
133	856078	48.1	2.42	13.5	12.7	0.21	6.97	12.5	2.44	0.28	0.27
137	855025	48.1	2.25	14.3	12.5	0.21	6.84	11.9	2.68	0.38	0.27
141	819023	48.5	1.74	14.7	11.3	0.15	7.57	13.0	2.32	0.20	0.16
142	799007	48.3	3.01	13.1	15.1	0.22	5.51	10.4	2.84	0.47	0.39
143	918077	48.6	1.79	13.9	12.7	0.22	7.13	12.5	2.25	0.12	0.16
mi1#	Midfell	48.5	0.76	15.5	9.17	0.18	9.74	15.5	1.54	0.01	0.04
mi2#	Midfell	48.7	0.76	15.5	9.21	0.17	9.58	15.3	1.55	0.01	0.03

Values in weight percent

*The sample locality coordinates are based on the UTM grid on the 1:50000 map sheets Hengill (1613 II) and Selfoss (1612 I). All samples are within UTM zone 27, and the complete reference to sample 1 is 27WMW831057.

+Total iron as FeO.

#Glass analyses of the picritic eruption unit at Midfell are given as mi1 and mi2 [*Risku-Norja*, 1985, Table 5].

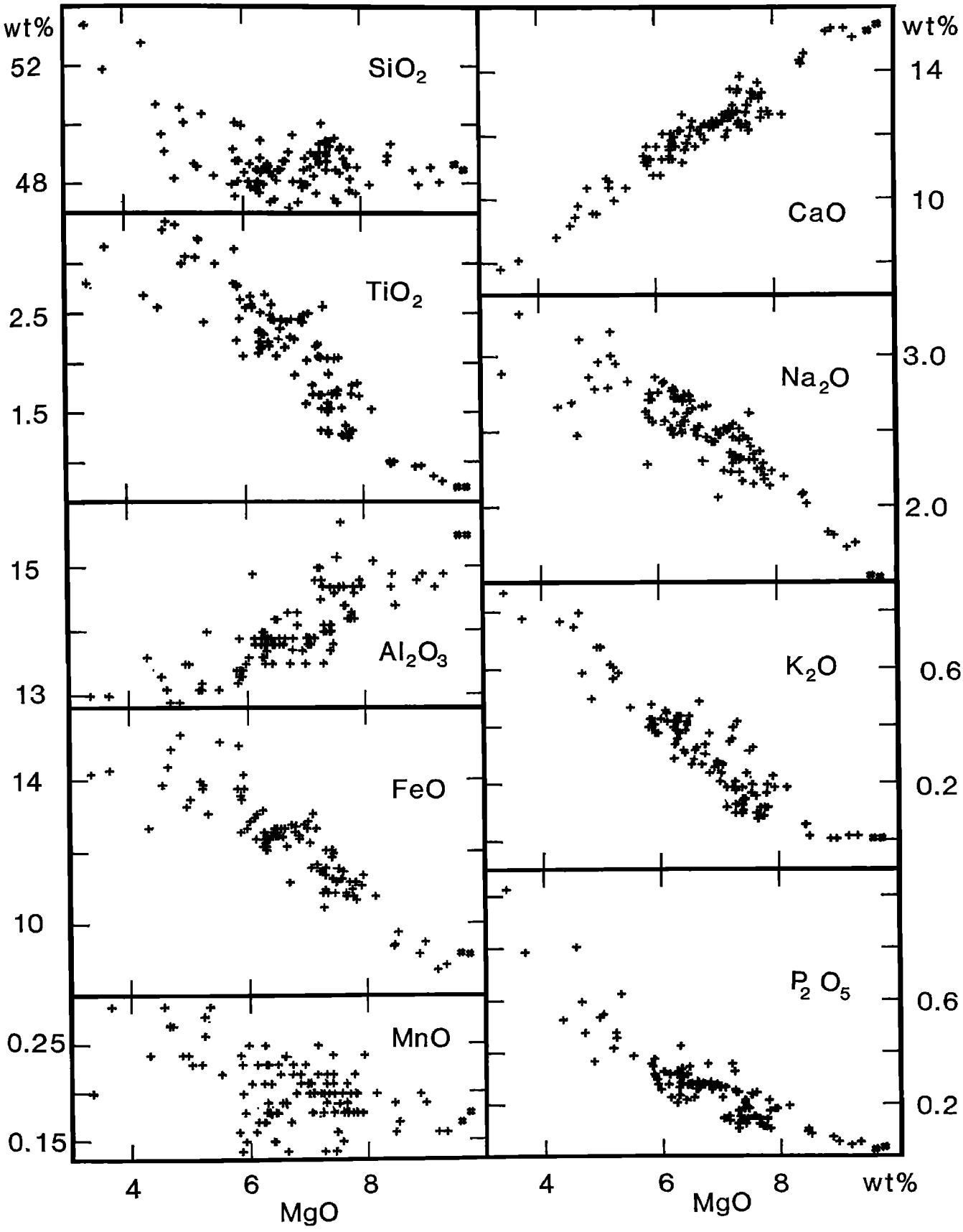

Fig. 5. Compositional variation diagrams for basaltic glasses from the Hengill volcanic system. Simple crosses are data from this study, and the two stars represent the analyses mi1 and mi2 from *Risku-Norja* [1985, Table 5].

SiO_2 shows very little variation for the glasses with more than 6 wt% MgO, but increases markedly with decreasing MgO-content below 5 wt% MgO.

The correlation between MnO and MgO is fairly poor, but MnO tend to vary in the same way as SiO_2.

The primitive olivine tholeiitic glasses from Midfell in the northeasternmost part of the Hengill system [*Risku-Norja*, 1985] define the least evolved end of the compositional spectrum. The samples from the eastern and the western subsystems of Hengill overlap completely on the variation diagrams. This indicates that the parental mantle derived magma as well as the nature of the crustal differentiation processes are similar in both of the subsystems.

Variation trends in basaltic glass composition similar to the Hengill trends are also found along the oceanic spreading ridges [e.g., *Melson et al.*, 1976, 1977; *Sigurdsson*, 1981] and in other Icelandic tholeiitic systems [*Grönvold and Mäkipää*, 1978; *Mäkipää*, 1978; *Grönvold*, 1984; *Meyer et al.*, 1985]. When plotted in MgO variation diagrams, the tholeiitic glasses from oceanic spreading centers and other Icelandic volcanic centers follow parallel and overlapping trends with the Hengill suite for most of the major elements. However, as shown in Figure 6 the Hengill suite is characterized by higher contents of CaO and lower contents of Al_2O_3 in glasses with more than 7 wt % MgO and by slightly lower SiO_2 content throughout the basaltic range, compared to the oceanic spreading center glasses. The difference in CaO and Al_2O_3 (almost 3 and 2 wt %, respectively, at 9 wt % MgO) is clearly significant and may indicate contrasting clinopyroxene and/or plagioclase control. The glass composition from other Icelandic tholeiitic centres generally fall between the Hengill and the mid-ocean ridge basalt (MORB) trends.

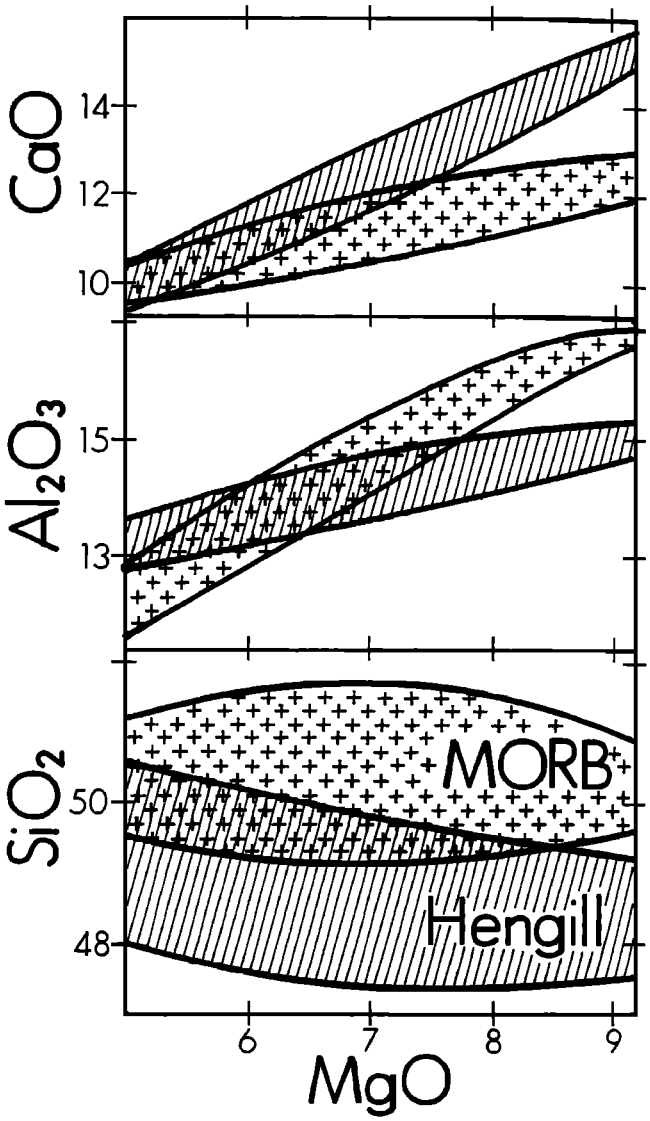

Fig. 6. Chemical variation range of CaO, Al_2O_3, and SiO_2 as a function of MgO for the basaltic glasses from Hengill and from oceanic spreading centers (MORB). The MORB variation is based on data from *Melson et al.* [1976, 1977], *Natland and Melson* [1980], *O'Donnell and Presnall* [1980], *Sigurdsson* [1981], and *Fujii and Bougault* [1983].

Phase Relations and Liquid Line of Descent

The Hengill glass compositions as well as the compositions of glasses saturated with plagioclase, olivine and clinopyroxene from melting experiments on basaltic compositions (references in Figures 7 and 8) were recast into simplified end-members and plotted in ternary projections of the pseudoquaternary system plagioclase(anorthite)-clinopyroxene-olivine-quartz(silica) according to the methods of *O'Hara* [1968], *Walker et al.* [1979], *Presnall et al.* [1979], *Grove et al.* [1982], and *Elthon* [1983]. The glasses in all of the eruption units from Hengill, except for the picritic units, are saturated with plagioclase, and the projection from plagioclase to the clinopyroxene-olivine-silica(quartz) pseudoternary plane is therefore most appropriate. The isomolar projection of *Elthon* [1983] is shown in Figure 7 along with the isostructural projections of *Walker et al.* [1979] and *Grove et al.* [1982] in Figure 8. All of the projections show that the evolved glasses of the Hengill spectrum follow closely the 1-atm olivine-plagioclase-clinopyroxene cotectic. The most primitive glasses, however, fall within the olivine-plagioclase primary phase volume. The compositions of primary melts in equilibrium with peridotitic residues at pressures of 1-20 GPa (experimental work cited in the captions of Figures 7 and 8) are invariably lower in the diopside component compared to the Hengill glasses. The most primitive mid-ocean ridge basalt glasses fall in the gap between the intermediate Hengill glasses and the 1-1.5 GPa primary melts.

The further discussion will be based mainly on Figure 7, since the isomolar projection method produces a good correlation between mole percent silica (in projection) and the degree of melt differentiation, e.g., in the form of 1/MgO or 1/CaO [*Elthon*, 1983]. The Hengill basaltic glass spectrum is divided into 4 compositional groups in Figure 7, and the chemical characteristics of each group are given in Table 4.

The following characteristics should be noted:

1. The group 1 glasses from the picritic eruption units fall well within the 1-atm olivine-plagioclase primary phase volume, indicating clinopyroxene undersaturation at low pressure. This is in accordance with the absence or ongoing resorption of clinopyroxene in these glasses.

2. Some group 2 glass compositions fall within the 1-atm olivine-plagioclase phase volume, and are compositionally similar to the most primitive MORB glasses (Figures 6 and 7).

3. The compositional spectrum of most of group 2 along with groups 3 and 4 follows the 1-atm plagioclase-olivine-clinopyroxene liquidus boundary and may be a result of low-pressure cotectic crystallization. The curvature of this boundary compared to the almost linear Hengill glass array may possibly indicate that some magma mixing indeed took place along the compositional spectrum. However, it is not possible to constrain the relative importance of fractionation and mixing on the basis of the pseudoliquidus diagrams.

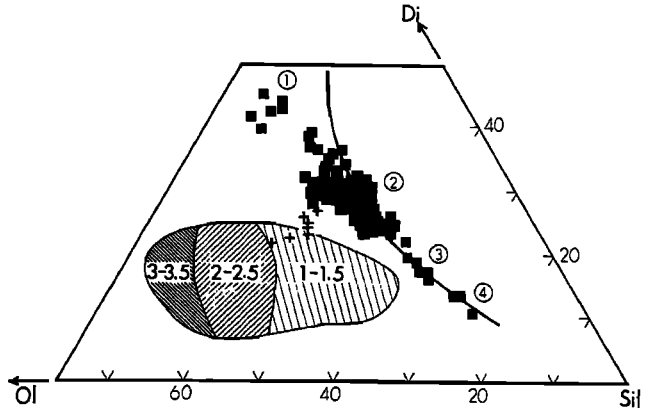

Fig. 7. Projection from anorthite(An) onto the olivine(Ol)-silica(Sil)-diopside(Di) plane in the pseudoquaternary system An-Ol-Sil-Di. Isomolar projection method of *Elthon* [1983]. The atomic $Fe^{3+}/(Fe^{2+}+Fe^{3+})$ is set to 0.07 in accordance with *Christie et al.* [1986]. Solid squares: Hengill basaltic glasses (103 analyses); crosses: primitive MORB glasses (seven analyses, four of which were used as starting materials in experimental studies of MORB: ALV 527-1-1[*Bender et al.*, 1978], DSPD 3-18-7-1[*Green et al.*, 1979], ALV 519-4-1[*Stolper*, 1980], and ARP 74-10-16, [*Fujii and Bougault*, 1983]. The three other analyses are listed as 18, 19, and 20 in Table 1.4.2.1 of *Basaltic Volcanism Study Project* [1981]); the hatched areas represent pseudoinvariant melt compositions in equilibrium with peridotitic assemblages and the numbers indicate the pressure ranges in gigapascal (data sources are *Stolper*, [1980], *Takahashi and Kushiro* [1983], *Elthon and Scarfe* [1984], *Fujii and Scarfe*, 1985; *Falloon and Green*, 1987; *Falloon et al.*, 1988]). The curved line is the 1-atm olivine-clinopyroxene cotectic of *Walker et al.* [1979] and *Grove and Bryan* [1983]. The numbers 1-4 indicate the compositional groups referred to in the text and in Table 4.

Major Element Mass Balance Calculations

Least squares mass balance calculations were carried out in order to assess the feasibility of deriving one liquid composition from another by subtraction of minerals in various proportions or by mixing with another melt composition. Both individual glass analyses (Table 3) and the averaged compositions of groups 1-4 (Table 4) were used in conjunction with experimentally produced and natural MORB glass compositions and the mineral compositions listed in Table 2. The results from the major element fractionation modelling are given in Table 5.

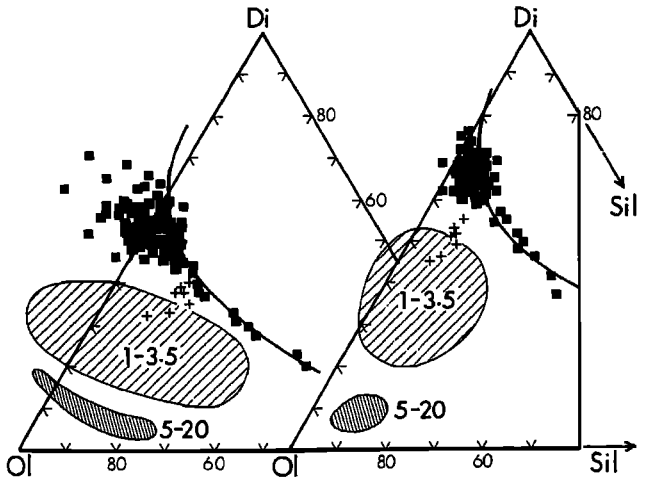

Fig. 8. Projections from plagioclase onto the Ol-Sil-Di plane using the following projection methods: (left) *Walker et al.* [1979] and (right) *Grove et al.* [1982]. The atomic $Fe^{3+}/(Fe^{2+}+Fe^{3+})$ is set to 0.07 in accordance with *Christie et al.* [1986]. Symbols as in Figure 6. Additional data sources for the 5-20 GPa pseudoinvariant melt compositions: *Takahashi and Scarfe* [1985], *Takahashi* [1986], and *Ito and Takahashi* [1987].

The most magnesian glasses of group 1 are the tentative first choice of parental melt composition of the Hengill suite. These compositions and the compositional line toward the group 2 compositions lie entirely within the low-pressure plagioclase-olivine primary phase volume. However, subtraction of various proportions of plagioclase and olivine from group 1 compositions to yield group 2 compositions fails to reproduce the observed CaO-Al_2O_3 variation. Removing CaO only in the form of plagioclase results in an insufficient decrease of the CaO content and an excessive decrease in the Al_2O_3 content. Introducing additional clinopyroxene in the fractionating assemblage greatly improves the situation, and a crystallizing assemblage of 10% olivine + 43% plagioclase + 47% clinopyroxene is a satisfactory solution (Table 5). This mineral assemblage is incompatible with low-pressure fractionation, indicating either that medium- to high-pressure fractionation, possibly in combination with magma mixing, was responsible for the melt evolution from group 1 to group 2 or that the group 1 compositions are not parental melts of the Hengill suite.

The melt evolution from group 2 to group 3 and from group 3 to group 4 can be reproduced by 49 and 30% fractionation of assemblages involving 10-17% olivine, 43-47% plagioclase, and 40-42% clinopyroxene (Table 5). This is consistent with the location of the intermediate and evolved glasses along the low pressure cotectic in Figure 7 and with the appearance of augite phenocrysts in some of the evolved glasses. Mass balance modelling also give excellent results for mixing of melts from groups 2 and 4 to form group 3 compositions, and the major element composition alone can therefore not constrain the mode of melt evolution.

The glasses of the picritic eruption units in Hengill (group 1) differ from primitive MORB glasses and melts in equilibrium with peridotitic residues at 1-2 GPa pressure by their higher calcium and normative diopside and their lower aluminum and normative plagioclase contents (Figures 6, 7, and 8). Mass balance modelling using melts equilibrated with peridotite at 1-2 GPa as parent liquids and the group 1 glasses as daughter liquids invariably requires a significant amount of clinopyroxene assimilation in combination with olivine and plagioclase fractionation (Table 5).

The process of clinopyroxene assimilation accompanied by olivine fractionation to form the primitive Hengill melts (Mælifell and Midfell eruption units) from mantle derived melts is supported by petrographic features of several of the eruption units. The chemical similarity between the abundant (25-30 vol %) plagioclase phenocrysts in several eruption units in the eastern subsystem and the cumulus plagioclase in the nodules from Tjarnarhnúkur and Midfell point to a nodule disintegration origin for many of the phenocrysts. Clinopyroxene phenocrysts are absent in the Tjarnarhnúkur lava and in other eruption units with more than 6 wt % MgO, except for the few markedly resorbed Al-Cr-endiopsides of the Mælifell and Midfell picrites. Direct textural evidence for disintegration of nodules and resorption of clinopyroxene can be found at Midfell [*Risku-Norja*, 1985] and Tjarnarhnúkur (Figure 4). The resorption of clinopyroxene is in accordance with the observation that the magnesian glasses have compositions that lie outside the low pressure phase volume of clinopyroxene.

The intermediate glass compositions of group 2 can be derived by fractionation of mainly olivine and plagioclase

TABLE 4*a*. Chemical Characteristics of the Four Compositional Basaltic Glass Groups of Figure 7

Group	Number of Samples	Silica in Isomolar Di-Fo-Sil Projection (Figure 7), mol %	CaO, wt %	MgO, wt %	K_2O, wt %
1	6	20-32	15.1-15.5	8.9-9.7	0.01-0.02
2	88	38-56	10.4-14.6	4.9-8.5	0.02-0.62
3	6	59-65	9.2-10.0	4.6-5.3	0.59-0.80
4	3	70-73	7.8-8.8	3.4-4.3	0.77-0.87

TABLE 4*b*. Average Group Composition and Standard Deviations

Group	SiO_2	TiO_2	Al_2O_3	FeO	MnO	MgO	CaO	Na_2O	K_2O	P_2O_5
1	48.4	0.86	15.1	9.12	0.18	9.29	15.3	1.71	0.01	0.05
	(0.0)	(0.10)	(0.4)	(0.27)	(0.02)	(0.34)	(0.1)	(0.13)	(0.01)	(0.02)
2	48.6	2.11	14.0	12.1	0.20	6.85	12.2	2.50	0.30	0.24
	(0.1)	(0.54)	(0.6)	(1.2)	(0.03)	(0.79)	(1.0)	(0.23)	(0.14)	(0.09)
3	50.1	2.98	13.4	13.9	0.27	4.86	9.61	2.84	0.68	0.60
	(0.1)	(0.41)	(0.4)	(0.7)	(0.03)	(0.29)	(0.28)	(0.23)	(0.08)	(0.11)
4	52.7	2.89	13.2	13.7	0.24	3.78	8.26	2.95	0.81	0.78
	(0.8)	(0.25)	(0.3)	(0.9)	(0.05)	(0.49)	(0.52)	(0.31)	(0.06)	(0.25)

Standard deviations are in parantheses

from experimentally produced melts in equilibrium with peridotitic residues at 1-2 GPa pressure (Table 5). Only minor amounts of clinopyroxene fractionation or assimilation is required in these models. In the isomolar projection in Figure 7 a large proportion of the group 2 glasses fall within the plagioclase-olivine phase volume, between the low pressure olivine-plagioclase-clinopyroxene cotectic line and the fields of melts in equilibrium with peridotitic residues at 1-2 GPa. The trail of the most primitive MORB compositions bridges the compositional gap between the experimental melts and the group 2 glasses.

The picritic eruption units comprising the group 1 glasses along with abundant olivine phenocrysts (20-30 vol %) and a few partly resorbed clinopyroxene xenocrysts are possibly not representative of parental magmas for the Hengill suite. Simple fractional crystallization at pressures of 0.2-0.6 GPa involving about 50% clinopyroxene in the fractionating assemblage may explain the evolution from group 1 to group 2 melts (Table 5). However, the absence of clinopyroxene phenocrysts and the compositional gap between group 1 and group 2 cast doubt on this model.

Basaltic Volcanism Study Project [1981, pp.153-154] and *Francis* [1986] pointed out the inconsistency between the need for clinopyroxene as a major fractionating phase in fractionation modelling of MORB, and the lack of clinopyroxene phenocrysts. This apparant discrepancy may be explained by fractionation of clinopyroxene at high pressure followed by mixing with more primitive melts and resorption of clinopyroxene [*Basaltic Volcanism Study Project*, 1981], or by compositional dispersion of olivine fractionation trends from picritic parental magmas between equilibrium and fractional crystallization [*Francis*, 1986]. Minor amounts of clinopyroxene assimilation in combination with olivine and plagioclase fractionation from melts in equilibrium with peridotitic residues at 1-2 GPa is also a viable mechanism for the generation of the primitive to intermediate portions of both the MORB and the Hengill glass spectra [*Trønnes*, 1987; *Bedard*, 1988]. The high Ca/Al ratios of all the group 1 glasses and many of the group 2 glasses are particularily difficult to explain without a significant uptake of clinopyroxene in these melts.

Trace Elements

Glass concentrates from 20 selected samples were analyzed for Rb, Sr, Y, Zr, and Ni (see the appendix), and the results are shown in Table 6 and Figure 9. The proposed fractionation from the melt compositions of group 2 to the compositions of groups 3 and 4 has been tested by Rayleigh and equilibrium fractionation modelling of the trace element evolution of the melts. The applied partitioning coefficients are listed in Table 7, and the results are shown in Figure 10. The average concentrations of groups 2 and 3 were used as starting compositions for the modelling. The mineral proportions of the fractionating assemblage were those derived by least squares mass balance modelling of the major element variation.

The observed trace element concentrations are generally in accordance with the predicted abundances from the modelling. The average concentrations of groups 3 and 4 fall within the range of predicted concentrations from the equilibrium and Rayleigh fractionation equations, respectively. The evolution from group 2 to group 3 requires a predominance of Rayleigh fractionation, especially for the compatible element Ni. The amount of fractionation derived from the major element mass balance calculations is also in reasonable agreement with the predicted evolution.

However, the evolution of the concentrations of Sr and Rb is problematic and requires further comments. The predicted growth of Sr is critically dependent on the choice of partitioning coefficient for Sr in plagioclase. If D_{Sr}(pl/melt) is greater than 2, the bulk distribution coefficient of Sr in the crystallizing assemblage will be near unity and the predicted evolution is an almost constant Sr content. This in conflict

TABLE 5. Results From Least Squares Mass Balance Fractionation Modelling Using Major Element Compositions.

Parent Composition	1	2	3	TK_1	$TK_{1,5}$	TK_2	ES_1	$ES_{1,5}$	ES_2	FS_1	TK_1	$TK_{1,5}$	TK_2	ES_1	$ES_{1,5}$	ES_2	FS_1
Daughter Composition	2	3	4	1	1	1	1	1	1	1	2	2	2	2	2	2	2
Percent crystallized	49	49	30	26	35	46	23	29	35	40-50	39	47	49	38	49	58	65-70
Subtracted Phases:																	
Olivine	5	5	5	12	19	31	9	15	20	12-16	14	20	23	10	17	22	15-20
Plagioclase	21	23	13	14	16	15	14	14	15	25-30	25	27	26	27	26	26	30-40
Clinopyroxene	23	21	12	--	--	--	--	--	--	-----	--	--	--	--	6	10	12-16
Percent Assimilated cpx	--	--	--	29	29	32	25	15	6	0-6	4	6	9	1	--	--	-----

The sums of the squared residuals (Σr^2) are less than 1.0 for the accepted solutions. Numbers 1-4: average compositions of groups 1-4 (Table 4). Quenched liquids coexisting with peridotitic residues: TK, *Takahashi and Kushiro* [1983]; ES, *Elthon and Scarfe* [1984]; FS, *Fujii and Scarfe* [1985]; the subscripts indicate pressure in gigapascal.

TABLE 6. Trace Element Content of Selected Glass Concentrates

Group	Sample	Rb	Sr	Zr	Y	Ni
1	66	ND	125	51	22	195
	73	ND	105	52	24	194
2	5	9	169	98	26	69
	22	9	153	77	25	104
	26	13	157	97	24	109
	32	12	206	144	28	94
	51	12	155	102	33	99
	53	10	182	95	31	95
	79	13	179	130	30	82
	100	16	155	81	33	79
	111	9	176	113	32	78
3	88	30	219	240	38	61
	89	28	233	303	70	39
	91	9	190	177	47	38
	109	8	173	138	58	49
4	46	18	212	317	64	34
	72	27	197	297	56	29
	90	10	227	345	66	27
5	9	56	180	933	145	19
	11	36	184	524	94	12

In ppm.

Group 5 is dacitic; the following major elements were determined by AAS (wt %): Sample 9, 0.5 MgO, 3.3 CaO, 4.6 Na_2O, 2.4 K_2O; Sample 11, 1.6 MgO, 4.7 CaO, 4.6 Na_2O, 1.6 K_2O. Range of MgO (wt %) within the other groups: Group 1: 9.3-9.0; group 2, 7.9-6.4; group 3, 5.8-4.6; group 4, 4.3-3.4.

with the observed increase in Sr with melt evolution within the basaltic range. A partition coefficient of 1.5 for Sr in plagioclase gives a reasonable fit between the observed and predicted evolution. A D_{Sr}(pl/melt) of 1.5 is in accordance with the data for lunar basalts at 1200°C of *Weill and MacKay* [1975], *McKay and Weill* [1976, 1977], and *Ringwood* [1970] and with the data of *Sun et al.* [1974] on MORB compositions, whereas the D_{Sr}(pl/melt) values of *Drake and Weill* [1975] are somewhat higher.

The Rb concentrations are problematic, partly since the analytical uncertainty for Rb (appendix) is about 40% of the total abundances for the samples of group 2 and some of the samples of groups 3 and 4. Whereas the samples in group 2 are characterized by uniform Rb contents of 9-13 ppm (sample 100 has 16 ppm Rb), the variations in groups 3 and 4 are very large (Figure 9). The samples of group 3 from the western subsystem (88 and 89) have much higher Rb content than the samples of group 3 and 4 from the eastern subsystem (especially samples 72, 91, and 109). The low-Rb samples define a possible fractionation trend. *Oskarsson et al.* [1982] determined the Rb contents of primitive olivine tholeiites from the Icelandic rift zones and found an average of 0.4 ppm Rb in the lavas with more than 9 wt % MgO. The same Rb content was found in the glass phase of the Midfell and Mælifell picrites [*Risku-Norja*, unpublished analyses, 1984, 1985). Crystal fractionation processes alone cannot account for the observed growth of Rb in the Hengill suite from such a low starting level. That would require unreasonably high degrees of fractionation (>97%) by either the Rayleigh or the equilibrium process and regardless of mineral proportions in

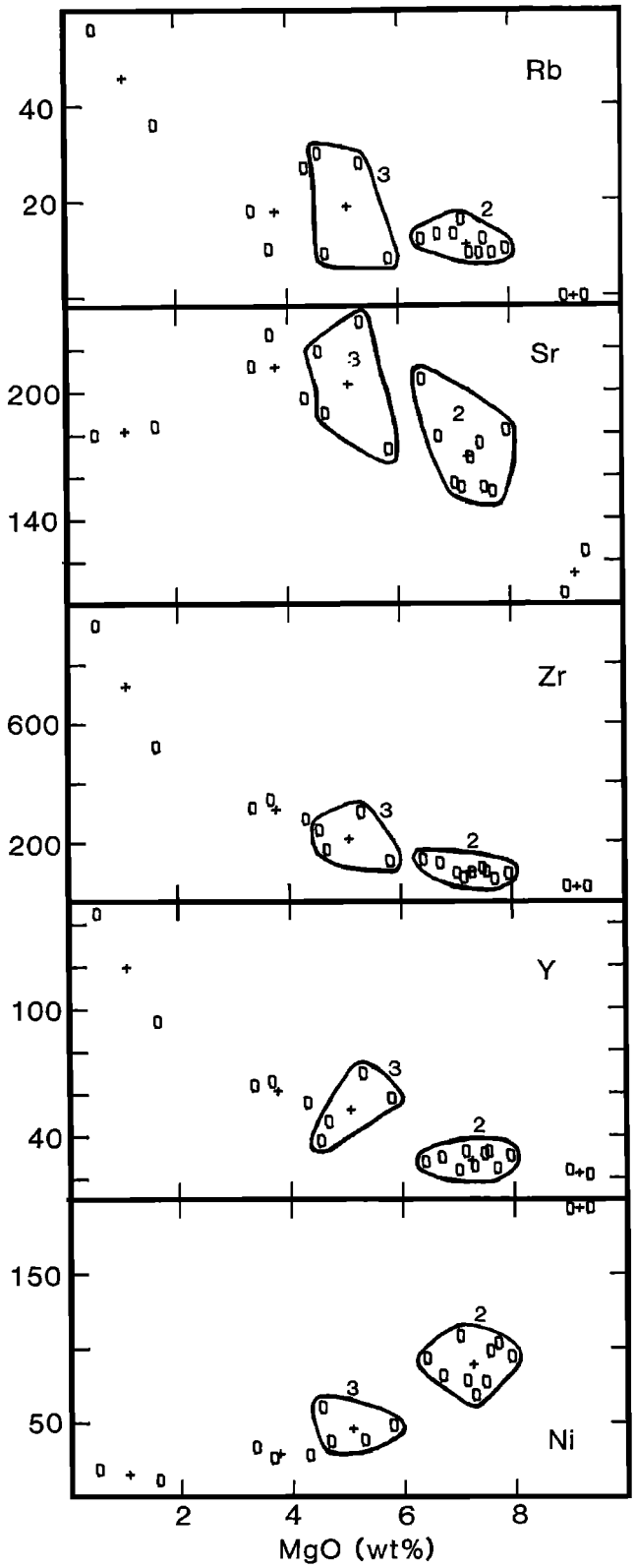

Fig. 9. Trace element variation (in ppm) versus MgO in the five compositional groups shown in Table 6. The circles are data points and crosses are the averages of each compositional group. The samples belonging to groups 2 and 3 are encircled.

the fractionating assemblage. Contamination of the mantle-derived magma with variable amounts of anatectic melts from the partly hydrated basalt lava pile is a reasonable mechanism for producing the high Rb contents.

TABLE 7. Mineral Melt Partition Coefficients Used for Modelling of Trace Element Fractionation

	Rb	Sr	Y	Zr	Ni	K	P
Pl	0.07	1.5	0.033	0.011	0.01	0.2	0.024
Ol	0.001	0.001	0.01	0.01	10.0	0.001	0.043
Cpx	0.001	0.07	0.55	0.1	2.0	0.002	0.009

The intermediate samples 88 and 89 from the western subsystem have apparantly undergone more extensive contamination (mixing) with crustal anatectic melts than the otherwise equally evolved samples 72, 91, and 109 from the eastern subsystem. The Rb-rich dacitic samples of group 5 as well as all known rhyolites exposed at the surface are also confined to the western subsystem. However, extensive contamination is not restricted to the western subsystem, since the Rb contents of samples 46 and 90 are also clearly elevated above the expected level of fractionation from a primitive mantle-derived parental magma. Even the Rb signatures of the group 2 melts are probably markedly influenced by crustal anatectic contamination.

Although the trace element variations within the Hengill suite conform with crystal fractionation as the dominating process of melt evolution, the data do not exclude magma mixing as an additional process. Mixing tests between groups 1 and 4 using the end member proportions derived from mass balance calculations result in average deviations of 8-25% for most of the elements. However, the calculated Ni concentrations are about 40% higher than the observed abundances, indicating that a considerable amount of fractionation of olivine and clinopyroxene is necessary.

MELT EVOLUTION, MAGMA DYNAMICS AND TECTONICS

Crustal Structure

Geophysical evidence indicate a general thinning of the Icelandic crust from an average thickness of 15-25 km under the Tertiary lava plateaus to about 10 km under the rift zones [*Björnsson*, 1984; *Björnsson*, 1985]. A low resistivity, partially molten layer at the base of the crust extending under most of Iceland has been detected by magnetotelluric measurements at about 70 sites [*Hermance et al.*, 1976; *Thayer et al.*, 1981; *Beblo and Björnsson*, 1978, 1980; *Beblo et al.*, 1983]. This layer has a well-defined upper limit but an unresolved and gradational lower part and has been interpreted as a partially molten zone at the base of the crust [*Schmeling*, 1985; *Tryggvason et al.*, 1983]. The depth to the lower crust (layer 3) under Iceland ranges from 3 to 6 km and is 3-4 km under the Hengill area [*Flovenz*, 1980]. Temperatures of 500-600°C are estimated for this transition zone beneath volcanic centers, and the boundary corresponds to the greenschist-amphibolite facies transition [*Oskarsson et al.*, 1982; *Flovenz*, 1980]. Crustal anatexis starts near the 650°C isotherm at about 5 km depth, marking the transition from low- to high-grade amphibolite facies [*Helz*, 1973, 1976; *Oskarsson et al.*, 1982]. Below this depth the mantle derived infrastructure in the form of cumulate-forming magma chambers, intrusive bodies and dikes makes up a rapidly increasing proportion of the crust at the expense of the subsiding metamorphosed lava pile.

Primitive Melts

The melt that accumulates beneath the lower crust of the rift zones has separated from the residual minerals of the mantle at

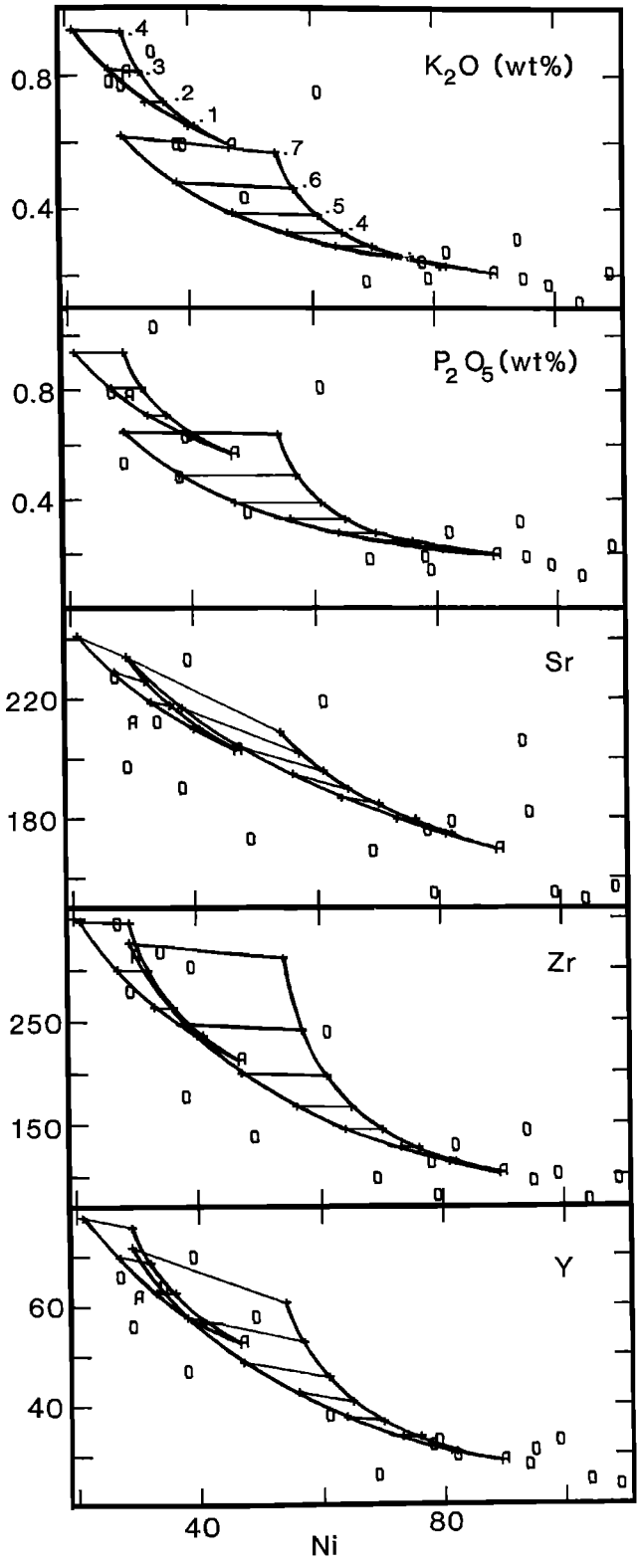

Fig. 10. Results from trace element fractionation modelling plotted in trace element variation diagrams with Ni as the abscissa. Values in ppm, except for K_2O and P_2O_5 (wt %). Average values for groups 2, 3, and 4 are shown with A, and the individual data points are shown with zeros. The models are based on the average values for group 2 and group 3 as starting compositions, the fractionating assemblages of Table 5, and the partition coefficients of Table 7. The lower curved heavy lines are the Rayleigh fractionation trends and the upper curved heavy lines are the equilibrium fractionation trends. The thin lines and numbers indicate the crystallized fractions.

depths of 10-50 km [*Schmeling*, 1985]. Although it is impossible to determine the exact depth of final equilibrium between the melt and the mantle residue, it is likely that the magmas that enter the crust have compositions similar to the subcrustal parental magmas of submarine oceanic spreading centres.

The pressure of formation and composition of primary MORB melts have been subject of much controversy [e.g., *O'Hara*, 1968; *Presnall et al.*, 1979; *Stolper*, 1980; *Takahashi and Kushiro*, 1983; *Elthon and Scarfe*, 1984; *Presnall and Hoover*, 1984,1986,1987; *Fujii and Scarfe*, 1985; *Elthon*, 1986]. However, *Klein and Langmuir* [1987], *Falloon and Green* [1988], and *Salters and Hart* [1989] provide strong evidence for a range of primary melt compositions generated from ascending peridotite sources througout wide pressure ranges of more than 2.5 GPa to less than 1 GPa.

Since the most magnesian glasses of the Hengill suite differ from primitive MORB glasses by their higher CaO and lower Al_2O_3 and since they must undergo fractional crystallization of mostly clinopyroxene to yield more evolved Hengill compositions, the parental nature of these melts is doubtful. Subcrustal melts of picritic compositions or compositions similar to primitive MORB melts can produce the melts of the Mælifell and Midfell eruption units by combined assimilation of clinopyroxene and fractionation of olivine and plagioclase. The selective assimilation of clinopyroxene is clearly a viable process in ascending magmas, since the primary phase volume of clinopyroxene decreases and the olivine volume increases with decreasing pressure.

Clinopyroxene is an important constituent in the cumulate sequences of the lower crustal sections of ophiolites. In the Oman ophiolite, for instance, the mineral is cumulus phase throughout the 3-5 km thick gabbro-dominated cumulate sequence, except for the lowermost 0-200 m where spinel (and chromite) bearing dunite is the dominating lithology [*Pallister and Hopson*, 1981]. The combined evidence from cumulate parts of ophiolites [e.g., *Coleman*, 1977; *Fox and Stroup*, 1981] indicate that melts fractionating under 0.2-0.3 GPa pressures in lower crustal magma chambers will reach the olivine-clinopyroxene-plagioclase cotectic after only a moderate amount of olivine + spinel (and chromite) deposition. If a primitive melt, undersaturated with clinopyroxene, but crystallizing olivine + spinel, ascends through parts of the solidified cumulate sequence, it is unlikely that interaction between the melt and wall rock clinopyroxene can be avoided. *Brearley and Scarfe* [1986] found that the relative rate of dissolution of the common peridotitic and gabbroic minerals is proportional to their relative stabilities as liquidus phases at various pressures. The dissolution rate of clinopyroxene is high at low pressures where clinopyroxene is not a liquidus phase.

There are several ways in which such an assimilation can occur. If the rate of magma flow through a dike exceeds a critical number, the flow will be turbulent, resulting in extensive thermal erosion of the walls of the dike [*Huppert and Sparks*, 1985; *Campbell*, 1985). It is unclear whether a dike flow rate sufficient for turbulence was attained during the eruption of the Maelifell and Midfell units. The 4-m average width of Icelandic dikes [*Gudmundsson*, 1986] seems insufficient for turbulent magma flow, but the relatively voluminous and primitive (partly picritic) eruptions, mainly in the form of lava shields from the latest glacial and early postglacial period, are probably the best candidates for dike turbulence.

Equilibrium assimilation of clinopyroxene will be a likely result of the accumulation of a primitive magma in a chamber or small reservoir within the partly solidified clinopyroxene bearing cumulate sequence. Addition of latent heat of crystallization from olivine + spinel fractionation to the heat

content of the magma and a wall rock at or near its solidus temperature will promote the assimilation. The textural evidence shown in Figure 4 indicates that clinopyroxene assimilation may also have occurred from xenoliths broken off from cumulate layers and transported upwards by the magma.

Eruption of Primitive Magmas

Gudmundsson [1986] suggested that the dense, primitive magmas erupt at the Reykjanes peninsula only during periods of favourable isostatic conditions of high pressure gradients extending from the crust to considerable depths in the mantle. The magmatic plumbing system under Pantelleria was also influenced by isostatic and sea level changes associated with the Pleistocene glacial cycles [*Wallmann et al.*, 1988]. The Pleistocene deglaciation events led to rebound of the glacially depressed Icelandic crust creating reduced pressure in the upper part of the subcrustal magma layer. The reduced pressure may have resulted in increased melt flow toward the rift zones both laterally from mantle areas near the periphery of, and possibly outside, the glacially depressed Icelandic landmass and vertically from deeper mantle areas. The crustal rebound model of *Gudmundsson* [1986] predicts tensional stresses in the lower crust in the flank zones of the central volcanoes, favouring the opening of dikes. The static magma overpressure (up to tens of megapascals) in the uppermost part of the mantle, produced by the pressure gradient, could drive dense magmas through the crust. The melts with the highest density were therefore erupted in the peripheral parts of the volcanic centers early in the rebound process, when the magma overpressure was near its maximum.

These model predictions are in accordance with field observations. At the Reykjanes peninsula the small picritic lava shields were formed earliest in the postglacial eruption sequence at the margins of the volcanic centers [*Jakobsson et al.*, 1978; *Gudmundsson*, 1986]. Likewise, the picritic Mælifell and Midfell eruption units, as well as a tuff ridge southwest of the Hengill mountain (8.5 wt % MgO in glass phase, samples 80 and 81), were erupted in the peripheral parts of the Hengill central volcano during the latest glacial stage.

The eruptions of larger olivine tholeiitic lava shields (up to 7 km^3 in volume) follow the earliest stage of picritic eruptions both at the Reykjanes peninsula and in the Hengill area [*Jakobsson et al.*, 1978; *Arnason et al.*, 1986]. These voluminous and fairly undifferentiated magmas (8-10 wt % MgO) were presumably driven to the surface by the residual magma overpressure. Large, monogenetic shield volcanoes of similar composition from the early postglacial (and interglacial) period are also found outside the central volcanoes along the Icelandic rift zones.

Ryan [1987] provided an alternative model for the effect of isostatic changes on magmatic plumbing systems in the crust. His "crustal contractancy" and "neutral buoyancy" concepts may also explain the invasion of voluminous and dense magmas at shallow levels during periods of glacial deloading. During a glacial period with extra loading of the crust, the contractancy effect will depress the neutral buoyancy level and effectively reduce the extent of the crustal magmatic infrastructure. The eruption rate in the Hengill area reached a minimum during the maximun Weichsel glaciation [*Arnason et al.* 1986], and the eruption products were more evolved, including dacites and rhyolites. This indicates that the supply of magma from the mantle was very reduced and large, stationary magma chambers were probably not present in the lower crust during the eruption of the primitive magmas accompanying the deglaciation.

Evolved Melts

In periods of stable lithostatic pressure conditions the dense, primitive magmas are not able to rise through the lighter crust and may be trapped near the floor of lower crustal magma chambers [*Huppert and Sparks*, 1980; *Sparks et al.*, 1980; *Stolper and Walker*, 1980]. Fractionation of olivine + spinel reduces the melt density, and the melt reaches the olivine + plagioclase + clinopyroxene cotectic simultaneously with a density minimum. At this point the melt has sufficiently high buoyancy to rise and mix with the overlying magma in the chamber [*Sparks et al.*, 1980; *Stolper and Walker*, 1980]. The gabbro-dominated cumulate layers of ophiolites indicate extensive cotectic crystallization at deep levels.

The group 2 glasses may represent melts erupted from these lower crustal magma chambers. However, even the group 2 glasses have Rb content above the concentrations expected from simple fractionation from mantle-derived melts, indicating some contamination by anatectic melts from the subsiding lava pile. This contamination may occur indirectly by mixing of the melts from the lowermost and totally mantle-derived crust with contaminated basaltic magma residing in shallower chambers.

Magmas rising buoyantly from magma reservoirs in the cumulate layer may become trapped at shallower levels where the surrounding crustal density decreases markedly. The level of incipient crustal anatexis and transition from low- to high-grade amphibolite facies (about 5 km depth) is an important level of change in both density and rheology. Immediately below this transition zone the subsiding crust will contain a significant proportion of interstitial anatectic melt and will behave more plastically than the cooler and more brittle crust above [*Marsh*, 1982; *Whitney and Stormer*, 1986]. It therefore appears likely that a considerable amount of slowly rising magma will be trapped at this level, and geopysical evidence for extensive midcrustal magma reservoirs under the currently active Krafla volcano is provided by *Einarsson* [1978] and *Tryggvason* [1986].

Further crystal fractionation in midcrustal reservoirs is promoted by mixing with cooler, silicic melts of anatectic origin [*Oskarsson et al.*, 1982]. The glasses of groups 3 and 4 probably represent melts at different evolutionary stages from midcrustal depths. The dacitic melts (group 5, Table 6, Figure 9) may either be formed by direct crustal anatexis or represent mixtures of basalt and anatectic rhyolite.

CONCLUSIONS

The isostatic conditions of the crust and upper mantle may partly control the volcanic eruption rate as well as the degree of evolution of the magmas admitted to the surface along the Icelandic rift zones. During peak glaciations (e.g., Weichsel) the excess lithostatic pressure and crustal "contractancy" [*Ryan*, 1987] supressed the magma supply from the mantle, resulting in small and infrequent eruptions of evolved magma, including the dacite and rhyolite units in the western Hengill subsystem. Lower crustal magma reservoirs were probably greatly reduced and possibly completely lost due to the low mantle magma supply.

The picritic eruption units (group 1 glass compositions) were formed at an early deglaciation stage. Their dense magmas were driven to the surface by the intermittant excess magma pressure and the elevated neutral buoyancy level. The glass composition of the picritic units is characterized by high calcium and low aluminum contents relative to primitive

MORB glasses with similar magnesium content. Mass balance modelling and the liquidus phase relations in the pseudoquaternary system olivine-diopside-plagioclase-silica indicate that these glasses can be produced by clinopyroxene assimilation combined with olivine and plagioclase fractionation from melts in equilibrium with peridotitic residues at 1-2 GPa pressure. Independent textural evidence in the form of resorbed clinopyroxene xenocrysts and partly disintegrated clinopyroxene-plagioclase nodules in highly plagioclase phyric lavas supports the clinopyroxene assimilation model.

Fractionation modelling of the evolution from the picritic magmas (group 1 melt compositions) to the intermediate basaltic melts (group 2 glasses) requires a clinopyroxene rich fractionation assemblage. However, the group 1 melts are clearly undersaturated with respect to clinopyroxene at low pressure, and the lack of evidence for clinopyroxene fractionation indicates that they may not be parental to the intermediate compositions. Olivine+plagioclase fractionation combined with minor assimilation or fractionation of clinopyroxene can produce the group 2 compositions directly from primary mantle-derived melts equilibrated with its peridotitic residues at pressures of 1-2 GPa. Minor amounts of clinopyroxene assimilation may also play an important role in the evolution of primitive MORB magmas.

Crystal fractionation (olivine, clinopyroxene, and plagioclase) at successively shallower levels combined with minor contamination with crustal anatectic melts explains both the major and trace element abundances of the intermediate and evolved basaltic glasses of the Hengill vocanic system.

APPENDIX: ANALYTICAL PROCEDURE

The major element compositions of unaltered glass fragments were determined by a wavelength dispersive electron microprobe on carbon-coated thin sections. The standard operating conditions, correction schemes, standardization, and counting statistics have been described by *Imsland* [1984], and the precision was comparable to that reported by *Thy* [1983]. A slightly defocussed electron beam and a sample current of 25 nA (exitation voltage of 25 kV) was used initially for all of the glasses, and those with more than 2.6 wt % Na_2O were reanalyzed with lower sample current (10-20 nA) and slowly moving sample relative to the stationary beam.

For each sample, 10-12 spot analyses were performed on different glass fragments and different parts of glass fragments. These analyses were collected in two series with several hours or days interval. Between each sequence of 5—15 spot analyses of one to three samples (20-60 min) two basaltic glass standards (WRAB-4; *B. Evans*, personal communication as cited by *Thy* [1983] and VG-A99 [*Jarosewich et al.* 1979]) were analyzed with two to three spot analyses on each. The average oxide contents of each sample series were adjusted according to the deviation between measured and accepted values of the standards.

Trace elements were analyzed in glass concentrates of 20 selected samples covering the major element compositional spectrum and containing none or very few microphenocrysts. The macrophenocrysts were removed by magnetic and heavy liquid separation methods combined with final handpicking under binocular microscope. Rb, Sr, Y, and Zr were analyzed by X-ray fluorescence spectroscopy using internal Mo-As standards and international reference standards, and Ni was analyzed by atomic absorption sectroscopy. The estimated precision and accuacy (one standard deviation) based on analyses of parallels and standards are 4 ppm for Rb, 14 ppm for Sr, 6 ppm for Y, 24 ppm for Zr, and 8 ppm for Ni.

Ackowledgements. This research was carried out during my tenure of a Nordic Council Fellowship and was financially supported by the Nordic Volcanological Institute. Karl Grönvold and Niels Oskarsson suggested a study of the Hengill system and provided field and analytical assistance. I thank them as well as A. Gudmundsson, V. Hardardóttir, H. Risku-Norja, K. Sæmundsson, G. Sigvaldason, the other institute members, and D. Caird for discussions and technical assistance. Further discussions with the late C.M. Scarfe, M.P. Ryan, E. Takahashi, and D.C. Presnall and reviews by K. Grönvold, H. Sigurdsson and an anonymous reviewer were also helpful. K. Grönvold and M. J. Carr provided computer programs.

REFERENCES

Arnason, K., G. I. Haraldsson, G. V. Johnsen, G. Thorbergsson, G. P. Hersir, K. Sæmundsson, L. S. Georgsson, and S. P. Snorrason, Nesjavellir: Jardfræði- og jardedlisfrædileg könnun 1985 (Nesjavellir: Geological and geophysical overview 1985), *Rep. OS-86014/JHD-02*, 125 pp., Natl. Energy Auth., Reykjavik, Iceland, 1986.

Basaltic Volcanism Study Project, *Basaltic Volcanism on the Terrestrial Planets*, 1286 pp,.Pergamon, New York, 1981

Beblo, M., and A. Bjornsson, Magnetotelluric investigation of the lower crust and upper mantle beneath Iceland, *J. Geophys., 45*, 1-16, 1978.

Beblo, M., and A. Bjornsson, A model of electrical resistivity beneath NE Iceland, correlation with temperature, *J. Geophys.,47*, 184-190, 1980.

Beblo, M., A. Bjornsson, K. Arnason, B. Stein, and P. Woldgram, Electrical conductivity beneath Iceland — Constraints imposed by magnetotelluric results on temperature, partial melt, crust and mantle stucture, *J. Geophys., 53*, 16-23, 1983.

Bedard, J. H., Magma chamber dynamics and recycling of crustal cumulates by the mantle: Evidence from Bay of Island Ophiolite, *Eos Trans. Am..Geophys. Union, 69*, 1476, 1988.

Bender, J. F., F. N. Hodges, and A. E. Bence, Petrogenesis of basalts from the project FAMOUS area: Experimental study from 0 to 15 kbars, *Earth Plant. Sci. Lett., 41*, 277-302, 1978.

Björnsson, A., Dynamics of crustal rifting in NE Iceland, *J. Geophys. Res., 90*, 10,151-10,162, 1985.

Björnsson, A., J. Tomasson, and K. Saemundson, Hengilssvædid: Stada jardhitarannsókna vorid 1974 (The Hengill area, the state of geothermal research, spring 1974), *Rep. OS JHD 7415*, 11 pp., Natl., Energy Auth., Reykjavik, Iceland, 1974.

Björnsson, S., Crust and upper mantle beneath Iceland, Structure and Development of the Greenland-Scotland Ridge, edited by M. H. P. Bott, S. Saxov and M. Talwani, *NATO Conf. Ser. 4, 8*, 31-61, 1984.

Bott, M. H. P., and K. Gunnarsson, Crustal structure of the Iceland-Faeroe Ridge, *J. Geophys., 47*, 221-227, 1980.

Brearley, J., and C. M. Scarfe, Dissolution rates of upper mantle minerals in an alkali basalt melt at high pressure: An experimental study and implications for ultramafic xenolith survival, *J. Petrol., 27*, 1157-1182, 1986.

Bryan, W. B., Regional variation and petrogenesis of basalt glasses from the FAMOUS area, Mid-Atlantic Ridge, *J. Petrol., 20*, 293-325, 1979.

Bryan, W. B., Systematics of modal phenocryst assemblages in submarine basalts: Petrologic implications, *Contrib. Mineral. Petrol., 83,* 62-74, 1983.

Campbell, I. H., The difference between oceanic and continental tholeiites: A fluid dynamic explanation, *Contrib. Mineral. Petrol. 91,* 37-43, 1985.

Carmichael, I. S. E., F. J. Turner, and J. Verhoogen, *Igneous Petrology,* 739 pp, McGraw-Hill, New York, 1974.

Coleman, R. G., *Ophiolites,* 220 pp., Springer-Verlag, New York, 1977.

Christie, D. M., I. S. E. Carmichael, and C. H. Langmuir, Oxidation states of mid-ocean ridge basalt glasses, *Earth Planet. Sci Lett., 79,* 397-411, 1986.

Drake, M. J., and D. F. Weill, The partition of Sr, Ba, Ca, Y, Eu^{3+} and other REE between plagioclase feldspar and magmatic silicate liquid: An experimental study, *Geochim. Cosmochim. Acta, 39,* 689-712, 1975.

Einarsson, P., S-wave shadows in the Krafla Caldera in NE-Iceland: Evidence for a magma chamber in the crust, *Bull. Volcanol., 41,* 187-195, 1978.

Elthon, D., Isomolar and isostructural pseudo-liquidus diagrams for oceanic basalts, *Am. Mineral., 68,* 506-511, 1983.

Elthon, D., Comments on "Composition and depth of origin of primary mid-ocean ridge basalts" by D.C. Presnall and J.D. Hoover, *Contib. Mineral. Petrol. 94,* 253-256, 1986.

Elthon, D., and C. M. Scarfe, High-pressure phase equilibria of a high-magnesia basalt and the genesis of primary oceanic basalts, *Am. Mineral., 69,* 1-15, 1984.

Falloon, T. H., and D. H. Green, Anhydrous partial melting of MORB pyrolite and their peridotite compositions at 10kb: Implications for the origin of primitive MORB glasses, *Mineral. Petrol., 37,* 181-219, 1987.

Falloon, T. H., and D. H. Green, Anhydrous partial melting of peridotite from 8 to 35kb and the petrogenesis of MORB, *J. Petrol. Spec. Lithosphere Issue,* 379-414, 1988.

Falloon, T. J., D. H. Green, C. J. Hatton, and K. L. Harris, Anhydrous partial melting of a fertile and depleted peridotite from 2 to 30 kb and application to basalt petrogeneis, *J. Petrol., 29,* 1257-1282, 1988.

Flovenz, O. G., Seismic structure of the Icelandic crust above layer three and the relation between body wave velocity and the alteration of the basaltic crust, *J. Geophys., 47,* 211-220, 1980.

Foulger, G. R., Hengill triple junction, SW Iceland, 1, Tectonic structure and the spatial and temporal distribution of local earthquakes, *J. Geophys. Res., 93,* 13,493-13,506, 1988a.

Foulger, G. R., Hengill triple junction, SW Iceland, 2, Anomalous earthquake focal mechanism and implications for process within the geothermal reservoir and at accretionary plate boundaries, *J. Geophys. Res., 93,* 13,507-13,523, 1988b.

Fox, P. J., and J. B. Stroup, The plutonic foundation of the oceanic crust, in *The Sea, vol. 7, The Oceanic Lithosphere,* edited by C. Emiliani, pp. 119-218, John Wiley, New York, 1981.

Francis, D., The pyroxene paradox in MORB glasses — A signature of picritic parental magmas?, *Nature, 319,* 586-589, 1986.

Fujii, T., and H. Bougault, Melting relations of a magnesian abyssal tholeiite and the origin of MORBs, *Earth Plant. Sci. Lett., 62,* 283-295, 1983.

Fujii, T., and C. M. Scarfe, Composition of liquids coexisting with spinel lherzolite at 10 kbar and the genesis of MORBs, *Contrib. Mineral. Petrol., 90,* 18-28, 1985.

Green, D. H., W. O. Hibberson, and A. L. Jaques, Petrogenesis of mid-ocean ridge basalts, in: *The Earth: Its Origin, Structure and Evolution,* edited by M. W. McElhinny, pp. 265-299, Academic, San Diego, Calif., 1979.

Grönvold, K., Myvatn fires 1724-1729, chemical composition of the lava, *Nord. Volcanol. Inst. Prof. Pap., 8401,* 1984.

Grönvold, K., and H. Mäkipää, Chemical composition of Krafla lavas 1975-1977, *Nord. Volcanol. Inst. Prof. Pap., 7816,* 1978.

Grove, T. L., and W. B. Bryan, Fractionation of pyroxene-phyric MORB at low pressure: An experimental study, *Contrib. Mineral. Petrol., 84,* 293-309, 1983.

Grove, T. L., D. C. Gerlach, and T. W. Sando, Origin of calc-alkaline series lavas at Medicine Lake volcano by fractionation, assimilation and mixing, *Contrib. Mineral. Petrol., 84,* 293-309, 1982.

Gudmundsson, A., Mechanical aspects of Postglacial volcanism and tectonics of the Reykjanes Peninsula, southwest Iceland, *J. Geophys. Res. 91.* 12,711-12,721, 1986.

Hardardóttir, V., The petrology of the Hengill volcanic system, southern Iceland, M.Sc. thesis, 260 pp., McGill Univ., Montreal, 1983.

Hardardóttir, V., The petrology of the Maelifell picrite basalt, southern Iceland, *Jökull, 36,* 31-40, 1986.

Helz, R. T., Phase relations of basalts in their melting range pH_2O=5 kb as a function of oxygen fugacity, I, Mafic phases, *J. Petrol., 14,* 249-302, 1973.

Helz, R. T., Phase relations of basalts in their melting ranges at p_{H_2O}=5 kb, II, Melt compositions, *J. Petrol., 17,* 139-193, 1976.

Hermance, J. R., R. E. Thayer, and A. Björnsson, The telluric-magnetotelluric method in the regional assessmant of geothermal potential, in *Proc. 2nd. UN Symp. Dev. Use Geotherm. Resour.,* 2, 1037-1048, 1976.

Huppert, H. E., and R. S. J. Sparks, Restrictions on the compositions of mid-ocean ridge basalts: a fluid dynamical investigation, *Nature, 286,* 46-48, 1980.

Huppert, H. E., and R. S. J. Sparks, Cooling and contamination of mafic and ultramafic magma during ascent through continental crust, *Earth Planet. Sci. Lett., 74,* 371-386, 1985.

Imsland, P., Iceland and the ocean floor: Comparison of chemical characteristics of the magmatic rocks and some volcanic features, *Contrib. Mineral. Petrol., 83,* 31-37, 1983.

Imsland, P., Petrology, Mineralogy and Evolution of the Jan Mayen Magma System, *Visindafelag Isl., Spec. Publ., 43,* 332 pp., 1984.

Irvine, T. N., and W. R. A. Barager, A guide to the chemical classification of the common volcanic rocks, *Can. J. Earth Sci., 8,* 523-545, 1971.

Ito, E., and E. Takahashi, Melting of peridotite at uppermost lower-mantle conditions, *Nature, 328,* 514-517, 1987.

Jakobsson, S. P., J. Jonsson, and F. Shido, Petrology of the western Reykjanes peninsula, Iceland, *J. Petrol., 19,* 669-705, 1978.

Jarosewich E., A. S. Parkes, and L. B. Wiggins, Microprobe analyses of four natural glasses and one mineral: An interlaboratory study of precision and accuracy, *Smithson. Contrib. Earth Sci., 22,* 53-67, 1979.

Klein, E. M., and C. H. Langmuir, Global correlation of ocean ridge basalt chemistry with axial depth and crustal thickness, *J. Geophys. Res., 92,* 8089-8115, 1987.

Lipman, P. W., N. G. Banks, and J. M. Rhodes, Degassing induced crystallization of basaltic magma and effects on lava rheology, *Nature, 317,* 604-607, 1985.

Mäkipää, H., Petrological relations in some Icelandic hyaloclastites, *Bull. Geol. Soc. Finl., 50,* 81-112, 1978.

Marsh, B. D., On the mechanics of igneous diaprirism, stoping, and zone melting, *Am. J. Sci., 282,* 808-855, 1982.

McKay, G. A., and D. R. Weill, Petrogenesis of KREEP, *Proc. Lunar Sci Conf.7th.,* 2428-2447, 1976.

McKay, G. A., and D. R. Weill, KREEP petrogenesis revisited, *Proc. Lunar Sci. Conf. 8th.,* 2339-2355, 1977.

Melson, W. G., T. L. Vallier, T. L. Wright, G. Byerly, and J. Nelsen, Chemical diversity of abyssal volcanic glass erupted along Pacific, Atlantic, and Indian Ocean seafloor spreading centers, in *The Geophysics of the Pacific Ocean Basin and Its Margin, Geophys. Monogr. Ser.,* vol. 19, edited by: G. H. Sutton et al., pp. 351-367, AGU, Washington, D. C., 1976.

Melson, W. G., G. R. Byerly, J. A. Nelsen, T. O'Hearn, T. L. Wright, and T. Vallier, A catalog of the major element chemistry of abyssal volcanic glasses, *Smithson. Contrib. Earth Sci., 19,* 31-60, 1977.

Meyer, P. S., H. Sigurdsson, and J. G. Schilling, Petrological and geochemical variations along Iceland's neovolcanic zones, *J. Geophys. Res., 90,* 10,043-10,072, 1985.

Morse, S. A., Cation diffusion in plagioclase feldspar, *Science, 225,* 504-505, 1982.

Natland, J. H., and W. G. Melson, Compositions of basaltic glasses from the East Pacific Rise and Siqueiros Fracture Zone, near 9°N, *Initial Rep. Deep Sea Drill. Proj., 54,* 705-723, 1980.

O'Donnell, T. H., and D. C. Presnall, Chemical variations of the glass and mineral phases in basalts dredged from 25°-30°N along the Mid-Atlantic Ridge, *Am. J. Sci., 280A,* 845-868, 1980.

O'Hara, M. J., The bearing of phase equilibria studies in synthetic and natural systems on the origin and evolution of basic and ultrabasic rocks, *Earth Sci. Rev., 4,* 69-133, 1968.

Oskarsson, N., G. E. Sigvaldason, and S. Steinthórsson, A dynamic model of rift zone petrogenesis and the regional petrology of Iceland, *J. Petrol., 23,* 28-74, 1982.

Oskarsson, N., S. Steinthórsson, and G. E. Sigvaldason, Iceland geochemical anomaly: origin, volcanotectonics, chemical fractionation and isotope evolution of the crust, *J. Geophys. Res. 90,* 10,011-10,025, 1985.

Pálmason, G., Kinematics and heat flow in a volcanic rift zone, with application to Iceland, *Geophys. J. R. Astron. Soc., 33,* 451-481, 1973.

Pálmason, G., Model of crustal formation in Iceland and application to submarine mid-ocean ridges, in: *The Geology of North America, vol. M, The Western North Atlantic Region,* edited by P. R. Vogt, and B. E. Tucholke, Geological Society of America, Boulder, Colo., 1986.

Pallister, J. S., and C. A. Hopson, Semail ophiolite plutonic suite: field relations, phase variation, cryptic variation and layering, and a model of a spreading ridge magma chamber, *J. Geophys. Res., 86,* 2593-2644, 1981.

Presnall, D. C., and J. D. Hoover, Composition and depth of origin of primary mid-ocean ridge basalts, *Contrib. Mineral. Petrol., 87,* 170-178, 1984.

Presnall, D. C., and J. D. Hoover, Composition and depth of origin of primary mid-ocean ridge basalts — Reply to D. Elthon, *Contrib. Mineral. Petrol., 94,* 257-261, 1986.

Presnall, D. C., and J. D. Hoover, High pressure phase equilibrium constraints on the origin of mid-ocean ridge basalts, Magmatic Processes: Physiochemical Principles, edited by B. O. Mysen, *Spec. Publ. Geochem. Soc., 1,* pp. 75-89, 1987.

Presnall, D. C., J. R. Dixon, T. H. O'Donnell, and S. A. Dixon, Generation of mid-ocean ridge tholeiites, *J. Petrol., 20,* 3-35, 1979.

Ringwood, A. E., Petrogenesis of Apollo 11 basalts and implications for lunar origin, *J. Geophys. Res., 75,* 6453-6479, 1970.

Risku-Norja, H., Gabbro nodules from a pricritic pillow basalt, Midfell, SW Iceland, *Nord. Volcanol. Inst. Prof. Pap., 8501,* 1985.

Ryan, M. P., Neutral buoyancy and the mechanical evolution of magmatic systems, Magmatic Processes: Physiochemical Principles, edited by B. O. Mysen, *Spec. Publ. Geochem. Soc., 1,* pp. 259-287, 1987.

Salters, V. J. M., and S. R. Hart, The hafnium paradox and the role of garnet in the source of mid-ocean-ridge basalts, *Nature, 342,* 420-422, 1989.

Sæmundsson, K., Vulkanismus und Tektonik des Hengill - Gebietes in Sudwest-Island. (Volcanology and tectonics of the Hengill area in SW Iceland). *Acta Nat. Isl., 2(7),* 109 pp., 1967.

Sæmundsson, K., Outline of the geology of Iceland, *Jökull, 29,* 7-28, 1979.

Sæmundsson, K., and S. Einarsson, Geological map of Iceland, sheet 3, SW Iceland, 2nd ed., Mus.Nat. Hist. and Iceland Geod. Surv., Reykjavík, 1980.

Schilling, J. G., Iceland mantle plume, *Nature, 246,* 141-143, 1973.

Schmeling, H., Partial melt below Iceland: A combined interpretation of siesmic and conductivity data, *J. Geophys. Res., 90,* 10,105-10,116, 1985.

Sigurdsson, H., First-order major element variation in basaltic glasses from the Mid-Atlantic Ridge: 29°N to 73°N, *J. Geophys. Res., 86,* 9483-9502, 1981.

Sparks, R. S. J., P. Meyer, and H. Sigurdsson, Density variations amongst mid-ocean ridge basalts: implications for magma mixing and the scarcity of primitive lavas, *Earth Planet. Sci. Lett., 46,* 419-430, 1980.

Stolper, E., A phase diagram for mid-ocean ridge basalts: Preliminary results and implications for petrogenesis, *Contrib. Mineral. Petrol., 74,* 13-27, 1980.

Stolper, E., and D. Walker, Melt density and the average composition of basalt, *Contrib. Mineral. Petrol., 74,* 7-12, 1980.

Sun, C.-O., R. J. Williams, and S.-S. Sun, Distribution coefficients of Eu and Sr for plagioclase-liquid and clinopyroxene-liquid equilibria in oceanic ridge basalts: An experimental study, *Geochim. Cosmochim. Acta, 38,* 1415-1433, 1974.

Takahashi, E., Melting of a dry peridotite KLB-1 up to 14GPa: Implications on the origin of peridotitic upper mantle, *J. Geophys. Res., 91,* 9367-9382, 1986.

Takahashi, E., and I. Kushiro, Melting of a dry peridotite at high pressures and basalt magma genesis, *Am. Mineral, 68,* 859-879, 1983.

Takahashi, E., and C. M. Scarfe, Melting of peridotite to 14 GPa and the genesis of komatiite, *Nature, 315,* 566-568, 1985.

Thayer, R. E., L. A. Bjornsson, L. Alvarez, and J. R. Hermance, Magma genesis and crustal spreading in the northern neovolcanic zone in Iceland: Telluric-magnetotelluric constraints, *Geophys. J. R. Astron. Soc., 65,* 423-442, 1981.

Thy, P., Phase relations in transitional and alkali basaltic glasses from Iceland, *Contrib. Mineral. Petrol., 82,* 232-251, 1983.

Trønnes, R. G., Melt evolution of an Icelandic rift zone volcano: Evidence for cpx-assimilation in primitive oceanic melts, in: *Symposium Troodos 87, Ophiolites and Oceanic Lithosphere,* Geological Survey Department, Nicosia, Cyprus, 1987.

Tryggvasson, E., Multiple magma reservoirs in an active rift zone volcano: ground deformation and magma transport

during the September 1984 eruption of Krafla, Iceland, *J. Volcanol. Geotherm. Res., 28,* 1-44, 1986.

Tryggvason, K., E. S. Huseby, and R. Stefansson, Seismic image of the hypothesized Icelandic hotspot, *Tectonophysics, 100,* 97-118, 1983.

Vink, G. E., A hotspot model for Iceland and the Voring Plateau, *J. Geophys. Res., 89,* 9949-9959, 1984.

Walker, D., T. Shibata, and S. E. DeLong, Abyssal tholeiites from the Oceanographer Fracture Zone, II, Phase equilibria and mixing, *Contrib. Mineral. Petrol., 70,* 111-125, 1979.

Wallmann, P. C., G. A. Mahood, and D. D. Pollard, Mechanical models for correlation of ring-fracture eruptions at Pantelleria, Strait of Sicily, with glacial sea-level drawdown, *Bull. Volcanol., 50,* 327-339, 1988.

Weill, D. F., and G. A. McKay, the partitioning of Mg, Fe, Sr, Ce, Sm, Eu and Yb in lunar igneous systems and a possible origin of KREEP by equilibrium partial melting, *Proc. Lunar Sci. Conf.6th.,* 1143-1158, 1975.

Whitney, J. A., and J. C. Stormer, Jr., Model for the intrusion of batholiths associated with the eruption of large-volume ash-flow tuffs, *Science, 231,* 483-485, 1986.

R.G. Trønnes, Department of Geology, University of Alberta, Edmonton, Alberta, Canada T6G 2E3

(Received July 24, 1989;
revised November 27, 1989;
accepted December 22, 1989.)